NATURAL BARRIERS THRUST

Yvonne Tsang, Natural Barriers Thrust

Lawrence Berkeley National Laboratory (LBNL)

Contact: 510.486.7047 | Yvonne_Tsang@ymp.gov

Introduction

For the Office of the Chief Scientist (an office within the Office of Civilian Radioactive Waste Management, U.S. Department of Energy), the Natural Barriers Thrust supports scientific studies of the natural system at the proposed repository site of Yucca Mountain. This natural system is composed of the unsaturated zone and the saturated zones at that site, and the hydrothermal-chemical environment within the emplacement drifts. The Natural Barriers Thrust stresses the realistic representation of the natural system with respect to processes and parameters, by means of laboratory, field, and modeling studies.

During the last 20 years, a substantial amount of research has been devoted to Yucca Mountain by the Office of Civilian Radioactive Waste Management (OCRWM). Site characterization of Yucca Mountain has been successfully carried out through experiments in tens of deep surface-based boreholes (reaching the water table), and in an underground facility. Extensive computational models have also been developed to simulate and understand the relevant processes at the site. However, in spite of the quantity of data collected and the knowledge acquired, the complexity of processes in the fractured rock, as well as the general scarcity of studies in the unsaturated zone fractured rock prior to the recent research on Yucca Mountain, make it necessary for the project to adopt significant conservatism in the Total System Performance Assessment (TSPA). This conservatism has been noted by many review committees. In an International Peer Review of the Yucca Mountain Project (YMP) TSPA for Site Recommendation, the Nuclear Energy Agency (NEA) of the Organization for Economic Cooperation and Development (OECD), and the International Atomic Energy Agency (IAEA), wrote that *(Total System Performance Assessment for the Site Recommendation (TSPA-SR)/OECD, Paris, 2002, page 12)*:

> ...demonstrating understanding should be complementary to demonstrating compliance and of at least equal importance. Two approaches are needed. The first is to present what is considered to be a realistic (i.e., nonconservative) analysis of the

likely performance of the repository using realistic assumptions and data….The second approach is an analysis for compliance purposes where conservative assumptions and parameter values are used to make the case more defensible.

More recently, NEA wrote (*Post-closure Safety Case for Geological Repositories, Nature and Purpose (OECD, Paris, 2004), pp. 43–44)*, regarding a TSPA analysis related to showing compliance:

> Due to the use of pessimistic parameter values and conservative assumptions, the performance of the repository is likely to be more favourable than that indicated by the analyses. Conservatism of the analyses constitutes an additional qualitative argument for safety, although conservatism in and of itself may also be interpreted as a lack of knowledge, and may thus detract from confidence. Conservatism is inevitable, and greatly to be preferred to optimism, but should be used and managed judiciously.

The Natural Barriers Thrust recognizes that conservatism may be interpreted as a lack of knowledge, and aims to reduce conservatism through increasing knowledge. We believe that if certain key conservatisms can be successfully addressed, it may be that it can then be shown that Yucca Mountain provides sufficient public health protection—even in the unlikely event that engineered systems have lost their integrity earlier than expected.

The proposed 2005 Environmental Protection Agency (EPA) two-tier standard with requirements beyond the original period of 10,000 years emphasizes the significance of the natural system's contribution to repository performance over geological time scales. Human civilization with recorded history has existed for approximately 10,000 years. On the other hand, geologic records over tens of thousands to millions of years are well established for natural attributes.

Basic Elements of the Natural Barriers Thrust

From the repository drifts to the accessible environment, the basic elements of the Natural Barriers Thrust are:

1. Drift Seepage
2. In-drift Environment
3. Drift Shadow
4. Unsaturated Zone (UZ) Flow and Transport
5. Saturated Zone (SZ) Flow and Transport.

As illustrated in Figure 1, the natural system components are interrelated and coupled to waste form and waste packages within the drifts, encompassing the unsaturated zone (UZ), through the saturated zone (SZ), to the compliance boundary, 20 km from the repository (where a well is schematically shown).

Drift Seepage

Representation of drift seepage and the amount and chemistry of water contacting waste packages and waste in the current Yucca Mountain approach is believed to be conservative. The Natural Barriers Thrust is investigating various ways of obtaining an improved understanding of the seepage process under different repository conditions. This effort includes enhanced data collection to reduce uncertainty, investigation of coupled processes during the thermal period, and the use of natural ventilation to greatly reduce or eliminate seepage.

- *Suppression of seepage by natural ventilation.* Ventilation and heat-induced circulation, caused by air-density variations resulting from temperature differences within drifts, can lead to evaporation and removal of moisture, preventing moisture from contacting waste packages. It is likely that these processes prevent drip formation and

thus seepage into the drifts, thus alleviating the need for costly in-drift engineered components.
- *Self-sealing due to chemical precipitation around the drift.* This results from coupled thermal, hydrological, chemical, and mechanical processes; it could change the flow pattern around the drift, greatly reducing seepage into drifts.

In-Drift Environment

The in-drift chemical environment plays a key role in determining the potential extent of waste package corrosion and the subsequent possibility of radionuclide release into the near-field rock. In the current Yucca Mountain Project approach, the coupled thermal, hydrological, and chemical processes within the drift are described by several zero- or one-dimensional models, which leads to multiple accounting of water available for waste dissolution and thus to a conservative representation of the drift barrier function in prevent-
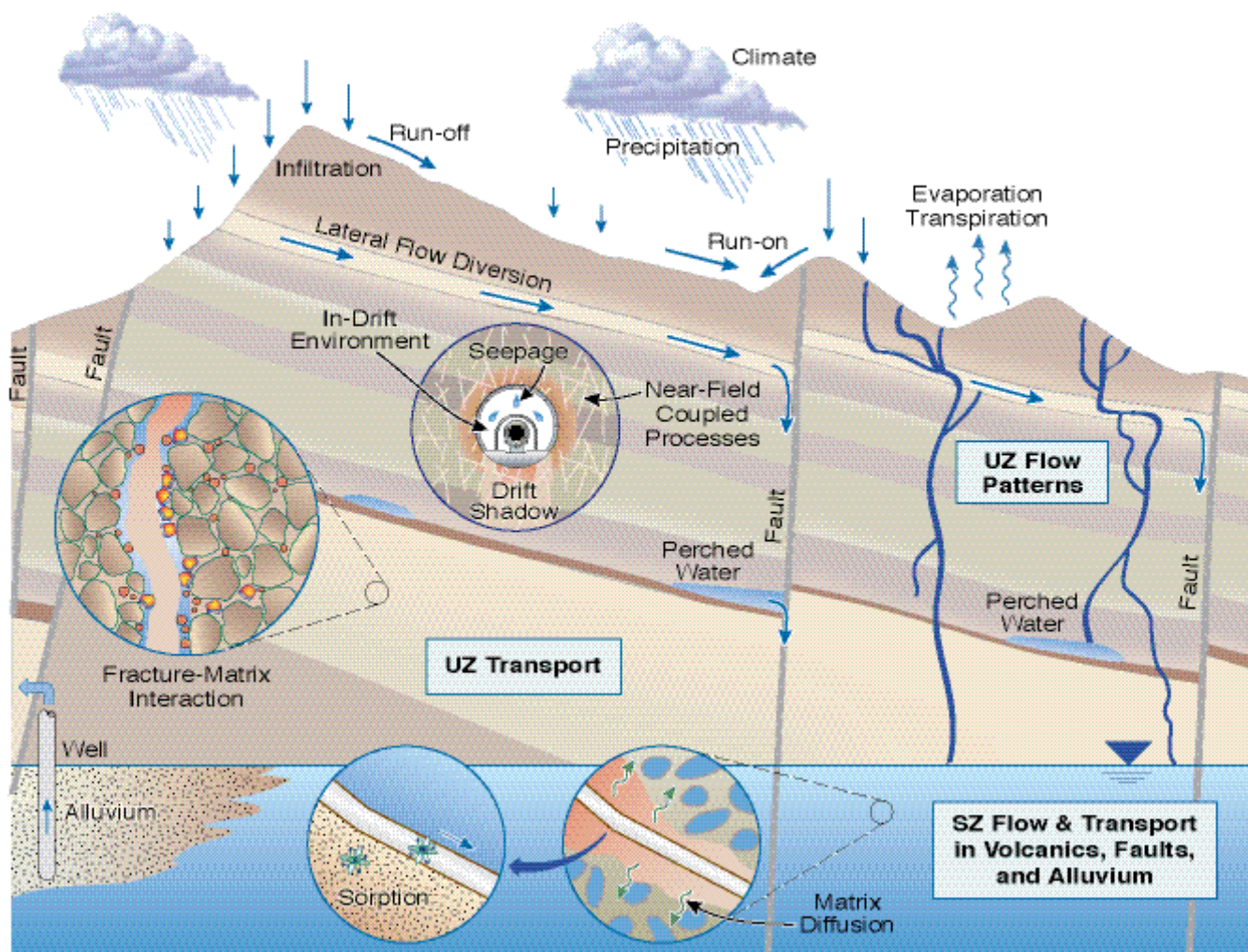

Figure 1. The Natural Barriers Thrust area.

ing release of radionuclides to the near-field rocks. The three science thrust areas described in this volume — Source Term, Materials Performance, and Natural Barriers — take an integrated approach toward investigating ways to remove the conservatism in the current project approach, thus achieving an improved representation of the drift barrier performance:

- *Integrated model to replace disjointed models:* The current approach of employing several disparate models, each describing an individual process — contributing discretely to (for example) the water composition of the end members, or salts on the waste package surfaces, or interactions with dust within the drift — limits the YMP's ability to address key questions concerning the in-drift chemical environment. A fully coupled approach that rigorously accounts for mass balance will improve the representation of the drift barrier function.

- *Coupling of in-drift transport with UZ processes in surrounding rocks.* There is currently no integrated treatment of transport of gas, vapor, or water between the near-field rocks and the waste emplacement drifts, nor within the drift. Capture of in-drift moisture transport along the drift into an enhanced model would enable realistic representation of evaporation and condensate movement.

Drift Shadow

The drift shadow is a region below a void in an unsaturated environment that is partially sheltered from downward-percolating water. It forms when the capillary forces are too weak to fully draw percolating water into the region. The drift shadow concept is not incorporated into the current Yucca Mountain approach, which assumes release of radionuclides into, and fast transport through, the fractures whenever seepage at the top of the drift occurs. The drift shadow concept, once demonstrated and validated, could greatly enhance repository performance by:

- *Delaying radionuclide release by thousands or tens of thousands of years.* Drift shadow is the natural consequence of water diversion around an underground opening (resulting from the negative capillary pressure in the rock), giving rise to greatly reduced water flux immediately below the opening — thus significantly limiting the mobility of radionuclides immediately below the drift.

- *Reducing peak dose potentially by orders of magnitude.*

Significantly reduced transport velocity in the shadow zone leads to delayed radionuclide breakthrough and reduced peak dose.

Unsaturated Zone (UZ) Flow and Transport

The UZ is the main natural-barrier component: it delays, retards, and sorbs radionuclides, and if represented realistically, can contribute to orders-of-magnitude dose reduction. The current Yucca Mountain representation of UZ transport is conservative. The Natural Barriers Thrust is investigating the different UZ retardation processes, with the aim of greatly reducing the uncertainty and conservatism of the present model:

- Effectiveness of matrix diffusion in retarding radionuclide transport

- Conservatism of the K_d approach and measurements based on crushed rock samples

- Other processes such as lateral diversion, permeability barriers below perched water bodies, and flow in faults.

Saturated Zone (SZ) Flow and Transport

Many processes that contribute to the SZ barrier function are represented conservatively in the current Yucca Mountain approach. Improved understanding of the SZ can greatly improve the description of the SZ barrier function, thus removing the overconservatism in the present project model description. The Natural Barriers Thrust addresses the following topics related to the SZ:

- *Determining if reducing conditions exist in the SZ for enhanced retardation.* One possible natural barrier to radionuclide migration in the SZ is the presence of nonoxidizing or reducing environments; the mobility of some radionuclides is known to greatly diminish in reducing groundwater.

- *Removing conservatisms in description of the retardation mechanisms.* Processes leading to retarded radionuclide transport include dilution, matrix diffusion, and sorption in the SZ.

The Natural Barriers Thrust places significant focus on the SZ to explore whether orders-of-magnitude dose reduction by dilution, diffusion, retardation, and other mechanisms can be demonstrated.

Progress in the Natural Barriers Thrust program of work through the first half of FY07 is reported in the pages that follow, addressing the above-listed scientific issues.

This page intentionally left blank.

DRIFT SEEPAGE

Thermal-Hydrological Near-Field Model Studies and Impact of Natural Convection on Seepage
George Danko, University of Nevada, Reno; Jens T. Birkholzer, Lawrence Berkeley National Laboratory (LBNL)

Integrated Assessment of Critical Chemical and Mechanical Processes Affecting Drift Performance: Laboratory and Modeling Studies
Derek Elsworth, Abraham S. Grader, Chris J. Marone, and Ki-Bok Min, Pennsylvania State University; Jonny Rutqvist and Eric Sonnenthal, Lawrence Berkeley National Laboratory (LBNL)

This page intentionally left blank.

Thermal-Hydrological Near-Field Model Studies and Impact of Natural Convection on Seepage

George Danko[1] and Jens T. Birkholzer[2]

[1]University of Nevada, Reno | [2]Lawrence Berkeley National Laboratory (LBNL)

Research Objectives

The heat output of the nuclear waste to be emplaced at Yucca Mountain will strongly affect the thermal-hydrological (TH) conditions in and near the geologic repository. While the rock mass heats up, the open drifts will act as important conduits for natural convection and ventilation processes. For example, as a result of natural convection driven by axial temperature gradients, water will evaporate from the drift walls in elevated-temperature sections of the drifts, migrate along the drifts, and condense in cooler sections (i.e., the end sections with no waste emplaced). Evaporation driven by natural convection may significantly reduce the moisture content in the near-drift fractured rock, which in turn can significantly reduce the potential for seepage of formation water into the drift. The research project described in this report aims at developing a multiscale, coupled seepage modeling approach that accounts for natural convection and ventilation. The potential of in-drift gas flows to remove moisture from emplacement drifts is examined, and the impact of axial moisture movement on seepage is determined.

Approach

A new seepage modeling approach is developed that accounts for the impact of evaporation caused by natural convection and ventilation processes. A simulation tool that aims to predict seepage rates affected by evaporation must address water, vapor, air, and heat transport in both the fractured rock mass and the open drift, and must handle the significant property differences between the two domains. In our approach, the flow and transport processes in the rock mass are simulated with the multiphase, multicomponent simulator TOUGH2 (Pruess et al., 1999), and the in-drift heat and moisture flows are simulated with the MULTIFLUX (MF) code (Danko et al., 2006). MF provides an efficient iterative coupling technique for matching the mass and heat transfer between the rock mass and the drift. To improve on the efficiency of the iterative coupling technique, MF applies a surrogate numerical transport code functionalization (NTCF) model (Danko, 2006) that periodically substitutes for TOUGH2 in the iterative solution process using surrogate response functions.

MF describes the relevant heat, moisture and air transport modes in the in-drift domain with a lumped-parameter CFD (Computational Fluid Dynamics) modeling approach. Various options are offered when configuring the coupled thermal-hydrologic air flow model. The lumped-parameter CFD model may be configured either for an open-volume drift air space that is connected to the ambient atmosphere, or for a closed-volume, pressure holding cavity. The transport of heat and moisture by laminar or turbulent air flow in the drift may be approximated as a dispersion process, with effective dispersion coefficients for heat and moisture, estimated via supporting CFD analyses from literature. Alternatively, the velocity distribution in the drift air space, and the transport of heat and moisture by laminar or turbulent convection, may be explicitly modeled in the lumped-parameter CFD model. The latter is a recent project development that significantly increases the applicability of the new model.

Accomplishments

Several research tasks have been accomplished to date. The coupled iterative solution procedure comprised of TOUGH2, MF, and NTCF elements has been developed and tested, and software qualification of the MF and NTCF elements is nearly completed. The new solution procedure has been applied to evaluate the heat-driven flow and transport processes in and near a representative waste emplacement drift at Yucca Mountain. One full emplacement drift was studied embedded in a monolithic, three-dimensional rock mass modeled in TOUGH2. The in-drift domain was initially modeled using a lumped-parameter CFD model in MF that describes the coupled laminar or turbulent air flow in the drift as a dispersion process, both above and below the drip shields (Danko et al., 2006). Several iterations were completed, refreshing the NTCF model against TOUGH2 runs. Figure 1 shows the 10th and 11th iteration results, confirming excellent convergence. Also shown for comparison are the results from an alternative model that uses a simplified in-drift model within TOUGH2.

The above application example was then simulated using a CFD configuration that solves explicitly for natural air flows in the drift air space. This model configuration offers two strategic advantages. First, because the in-drift air flows

are simulated as temporally and spatially vary-
ing processes, no prior knowledge of equivalent
dispersion coefficients is necessary. Second, as
the velocity distribution in the drift is explicitly
modeled, the complex flow patterns in the drift
are better represented. The second iteration
results of the new model are shown in Figure 1,
together with the previous "dispersion model"
results. The differences—higher temperature
and more moisture in the coldest drift segments
where no waste is emplaced—can be attributed
to the stronger air-flow circulation in the axial
drift direction. The results suggest that the new
model, because it includes physical processes
not heretofore considered, predicts more favor-
able conditions in the emplacement drift.

Another research task was initiated recently to
explicitly determine the impact of the in-drift
moisture transport on drift seepage. Because
seepage is driven by small-scale heterogeneities
in the rock mass, seepage simulations were con-
ducted at high resolution, with rock-mass
(sub)domains similar to previous seepage mod-
els (e.g., Birkholzer et al., 2004). The in-drift con-
ditions for the small-scale seepage model—most impor-
tantly the temperature and relative humidity conditions in
the drift—were provided by the full-scale in-drift results
shown in Figure 1. Average percolation fluxes were
increased by a factor of ten to represent a high-percolation
domain, where seepage is more likely. Example results are
presented in Figure 2, in the form of the saturation history

Figure 1. Drift wall temperature evolution at the hottest (a) and coldest (b) drift segments; and
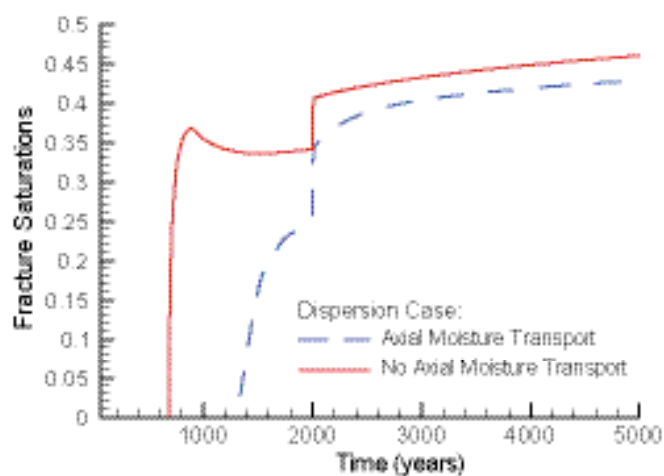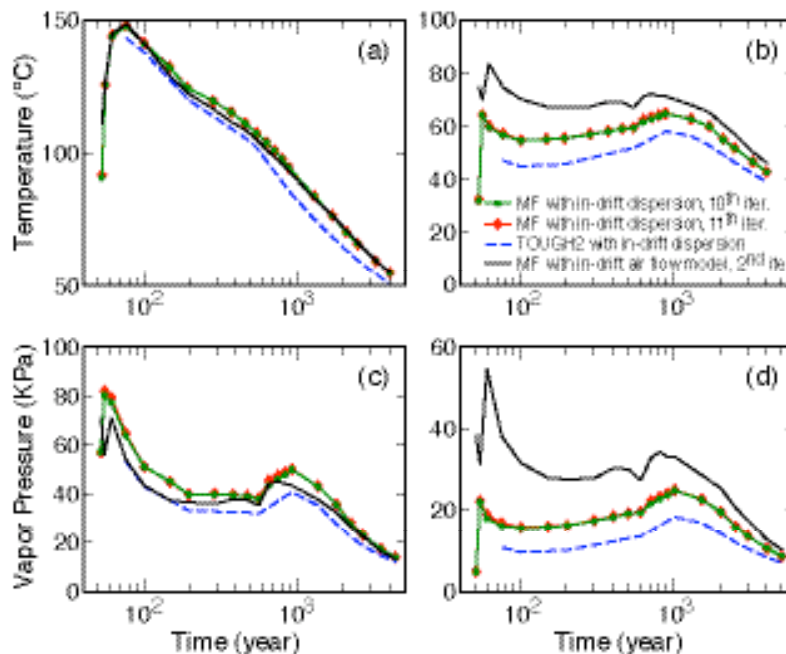vapor-pressure evolution at the hottest (c) and coldest (d) drift segments.

Figure 2. Saturation history at a potential seepage location in fractured rock near
drift crown, at hottest drift segment. Two simulation cases are considered: with
and without axial moisture transport. Percolation flux is increased by a factor of
ten.

at a potential seepage location in the rock mass near the
crown of the hottest drift segment. Earlier rewetting and
higher fracture saturations are predicted for the case in
which moisture transport along the drift axis is neglected,
which indicates a higher potential for seepage. Ongoing
work evaluates the seepage differences between models
with and without natural convection. Direct coupling of
the small-scale seepage model to MF, rather than using
predefined boundary conditions, is under way.

Related Publications

Birkholzer, J.T., S. Mukhopadhyay, and Y. Tsang, Modeling
    seepage into heated waste emplacement tunnels in
    Unsaturated Fractured Rock. Vadose Zone Journal, 3,
    819–836, 2004.
Danko, G., Functional or operator representation of
    numerical heat and mass transport models, Journal of
    Heat Transfer, 128, 162–175, February 2006.
Danko, G., D. Bahrami, and J.T. Birkholzer, The effect of
    unheated sections on moisture transport in the emplace-
    ment drift. Proceedings, Int. High-Level Radioactive
    Waste Management Conference, Las Vegas, 2006.
Pruess, K., C. Oldenburg, and G. Moridis, TOUGH2 User's
    Guide, Version 2.0. Report LBNL-43134, Lawrence
    Berkeley National Laboratory, Berkeley, California, 1999.

Integrated Assessment of Critical Chemical and Mechanical Processes Affecting Drift Performance: Laboratory and Modeling Studies

Derek Elsworth[1], Jonny Rutqvist[2], Ki-Bok Min[1], Abraham S. Grader[1], Chris J. Marone[1], and Eric Sonnenthal[2]
[1]Pennsylvania State University | [2]Lawrence Berkeley National Laboratory (LBNL)

Research Objectives

This work involves recovering unusually well-constrained laboratory data to define changes in the mechanical and transport properties of fractures as a result of hydrothermal conditions anticipated in the drift-local environment. These data will be incorporated into novel thermal-hydrological-mechanical-chemical (THMC) process simulators to evaluate the influence of strong couplings between stress and chemistry on drift performance.

Approach

We are examining the implication of critical coupled chemical-mechanical processes on drift performance at Yucca Mountain, through a coordinated suite of experimental and modeling studies.

Accomplishments

Activities have been divided between laboratory experiments to determine mechanical-chemical constitutive behavior, and modeling to upscale these results and to examine the resulting processes on drift performance.

Single direct shear experiments have been conducted on roughened planar surfaces of tuff to measure the evolution of permeability with shear loading. These experiments have returned peak friction coefficients on the order of μ ~0.6 and exhibit a slight reduction at maximum shear offset (~10 mm). Initial bulk permeabilities of the smooth fracture sample begin at k_b~10^{-14}–10^{-15} m^2 and decrease with an increase in initial normal stress, and with an increase in shear stress or shear offset. The decrease in permeability with shear offset results from the generation of wear products at the interface. These products are observed on the fracture surfaces at the completion of the test.

Constitutive modeling has focused on defining the mechanical and transport response of fractures to increasing stress and temperature,

and on implementing these preliminary representations in distributed parameter models (Elsworth and Yasuhara, 2006; Min et al., 2007). Few data are available to constrain such models. However, existing laboratory data and an understanding of critical processes have been used to develop preliminary constitutive models, supported by data from prior laboratory studies and from the results of a prior large-scale *in situ* block experiment (the TerraTek experiment at the Idaho Springs Mine, c. 1982).

The constitutive models incorporate the separate influences of stress and temperature in controlling changes in permeability, and are informed by laboratory data on novaculite. Importantly, these behaviors are capable of representing field observations in which fracture apertures are observed to decrease from 30 μm to 10 μm under constant stress, for an increase in temperature from 20° to 100°C—corresponding to a thirty-fold reduction in permeability under constant stress.

These behaviors have been incorporated into finite element models, to represent the thermo-mechanical response of the drift environment to combined thermal and stress effects. These include projections in permeabilities and the feedback on anticipated reductions in stresses over the case where these behaviors are not accommodated.

For typical drift-local conditions, permeabilities are shown to evolve as in Figure 1, representing a two-order-of-mag-
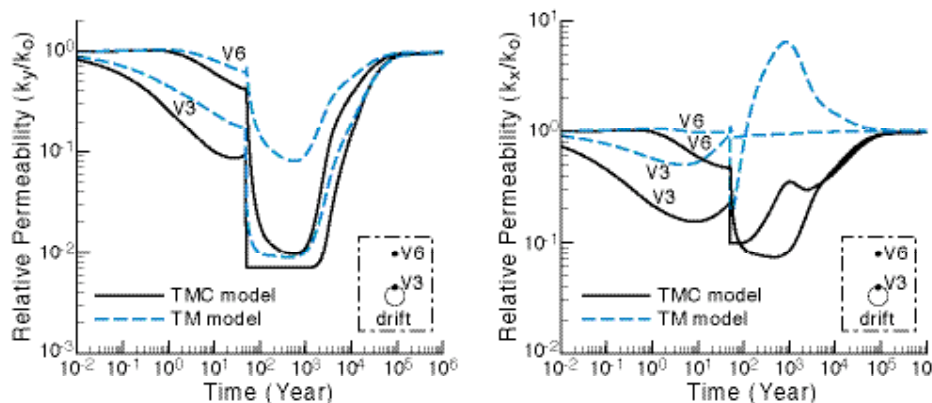

Figure 1. Comparisons of relative permeability evolution with (TMC) and without (TM) considering chemical strains at selected points. Relative changes in vertical (left) and horizontal (right) permeabilities. V3 is located at the top of the drift and V6 is located 10.75 m vertically above.

nitude change in permeability. Comparison of thermo-mechanical (TM) and thermo-mechanical-chemical (TMC) modeling shows that there can be up to a one-order-of-magnitude difference between the cases in which chemical effects are and in which they are not considered. The permeability is reduced more where chemical effects are considered together with mechanical effects, versus when they are not. The time to maximum reduction in permeability is concurrent with peak stress and temperature for the case of vertical permeability, which is most strongly influenced by changes in horizontal stress. Conversely, the evolution of vertical thermal stress is not straightforwardly related to temperature and makes the change in horizontal permeability dependent on relative local displacement constraints. Although changes caused by chemical strains will be irreversible, these current evaluations are merely reversible.

These interactions also change stress distribution. The thermal stress generated is smaller than where chemical effects are absent, because the reduction in aperture caused by temperature increase partially cancels the expansion of the intact rock. The overshoot in the reduction of stress upon cooling is explained by the irreversible change of aperture. What this behavior implies is important, since excess thermal stresses are reduced over anticipated magnitudes, and the ultimate reduction in stress may result in the loss of keying around underground excavations, where local failure may be more likely, owing to loss of confinement.

We are examining data from the Yucca Mountain Drift Scale Test (Rutqvist et al., 2007) for evidence of such effects. These include mismatches between anticipated and measured permeabilities, strains, and stresses. Such analyses are complicated by the concurrent influences of changing thermal-stress (TM) and water-saturation (TH) fields.Permeability data for the cooling phase have recently been evaluated, and we now have data for the entire 4 years of heating and subsequent 4 years of cooling.

Preliminary evaluations from the 46 measurement points, which are located at distances of between ~ 5 to 20 m away from the heated drift, are available. These evaluations indicate that permeabilities are depressed in the heating phase close to the heat source and recover slowly in the cooling phase, but suffer some irreversible changes. The maximum reduction in permeability is about one-
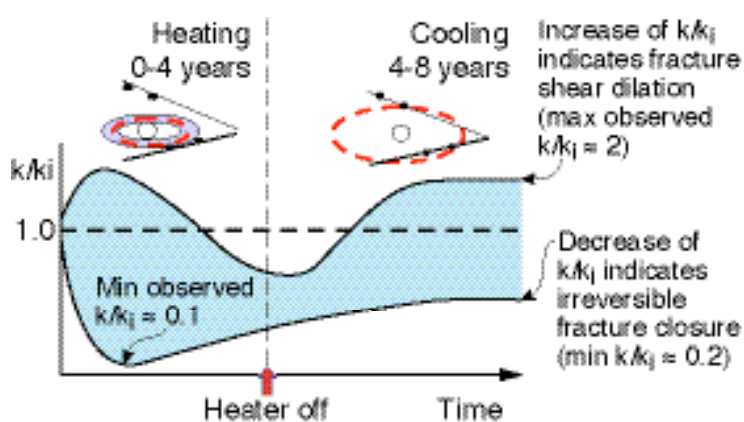

Figure 2. Schematic of observed changes in air-permeability at the Drift Scale Test during the 4-year heating period followed by a 4-year cooling period.

order-of-magnitude, and occurs during heating. At the end of cooling, the maximum permeability increase is a factor of 2, and the strongest permeability reduction is a factor of 0.2 of the original permeability. Thus, changes in permeability at the Drift Scale Test are limited to within one order of magnitude, as illustrated in Figure 2.

Importantly, the observed changes in permeability can only be explained by considering both TH and TM effects. The induced changes in permeability are within one order of magnitude (increase or decrease). Moreover, the permeability changes measured at the end of the cooling period likely reflect mechanically induced changes in permeability that might be mediated by chemo-mechanical effects. Displacement data are being examined to examine the causality of these observed permanent changes in permeability.

Related Publications

Elsworth, D., and H. Yasuhara, Mechanical and transport constitutive models for fractures subject to dissolution and precipitation. 2006 (submitted).

Min, K.-B., J. Rutqvist, and D. Elsworth, Chemically and mechanically mediated influences on the transport and mechanical characteristics of rock fractures. 2007 (submitted).

Rutqvist, J., et al. (2007) Analysis of coupled THM effects on permeability at the Yucca Mountain Drift Scale Test — Evidence of irreversible changes after heating and cooling in fractured rock. 2007 (in preparation).

In-Drift Environment

Coupling Thermal-Hydrological-Chemical (THC) Models to Process Models for Waste Packages
Guoxiang Zhang, Nicolas Spycher, Eric Sonnenthal, and Carl Steefel, Lawrence Berkeley National Laboratory (LBNL)

This page intentionally left blank.

Coupling Thermal-Hydrological-Chemical (THC) Models to Process Models for Waste Packages

Guoxiang Zhang, Nicolas Spycher, Eric Sonnenthal, and Carl Steefel
Lawrence Berkeley National Laboratory (LBNL)

Research Objectives

The main objective of this project is to develop an integrated, coupled thermal, hydrological, and chemical (THC) model of the near-field rock and in-drift environment at Yucca Mountain, to provide a link between the THC processes in the near field (evaluated under the Natural Barrier Targeted Thrust) and those taking place in waste-emplacement drifts, affecting waste package corrosion and fuel degradation (evaluated under the Materials Performance Targeted Thrust and Source Term Targeted Thrust). Specifically, this project aims to:

- Develop a quantitative model of coupled THC processes potentially leading to brine formation on top of waste packages and/or a drip shield.
- Dynamically integrate the model into the larger-scale process models within and around waste-emplacement tunnels, and into the smaller-scale waste-package corrosion models.

Approach

Process models were implemented into TOUGHREACT to allow modeling of evaporative concentration to very high ionic strength, boiling point elevation caused by dissolved salts, boiling/evaporation to dryness, and salt deliquescence (Zhang et al., 2006a, 2006b).

Using TOUGHREACT, we ran an integrated near-field/in-drift THC simulation using a vertical 2-D grid extending from near the ground surface to the groundwater table and covering a width equal to half the designed drift spacing of 81 m (a symmetrical model consistent with other ongoing near-field THC modeling investigations). A heterogeneous permeability field and high infiltration rates (10 times mean infiltration) were assumed, to ensure seepage into the drift. Starting water composition was taken from analyses of pore waters in Alcove-5 of the Exploratory Studies Facility (ESF). The geologic time period simulated was 600 years, with the boiling front collapsing at ~250 years, followed by in-drift seepage.

The integrated model was then used to simulate a discrete dripping event within the drift. At first, interactions with the waste source were not considered. The model was then refined to consider the release of radionuclides (representatively, UO_2^{+2} and NpO_2^{+2}) into seepage water as this water contacts the waste package and flows through the invert. (The oxidation of the waste form to UO_2^{+2} and NpO_2^{+2} was not explicitly modeled.) The precipitation of uranophane ($Ca(UO_2SiO_3OH)_2 \cdot 5H_2O$) and Np-uranophane was also considered. These minerals form in the invert from the neutralization of mildly acidic seepage water by clay minerals.
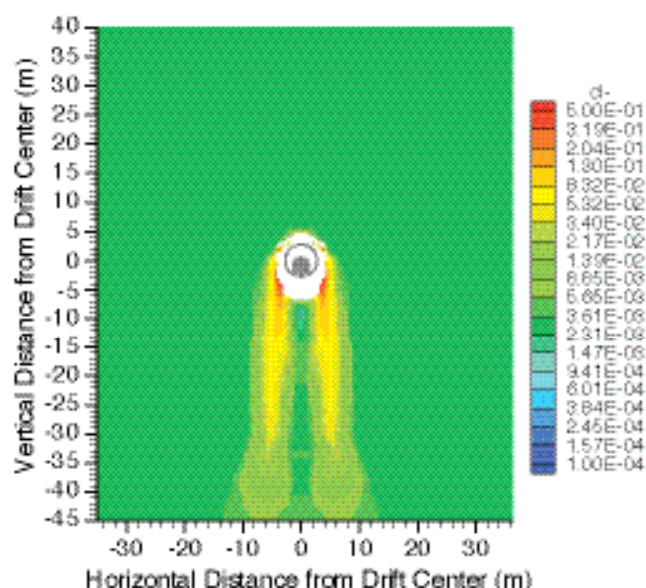

Figure 1. Simulated distribution of chloride concentrations during the collapse of the boiling front (at ~300 years) showing "shedding" of mildly concentrated waters resulting from the dissolution of previously precipitated salts in the dry-out zone.

Accomplishments

Model results provide information of direct interest to the Natural Barrier, Materials Performance, and Source Term Thrusts. Preliminary integrated simulations indicate:

- The near-field and in-drift brine chemical evolution is dominated by the precipitation of NaCl, $CaSO_4$, and $CaCO_3$.

- Rewetting of salts during collapse of the boiling front yields chloride concentrations <~20 x ambi-

ent values in waters percolating back towards the drift (Figure 1).

- The generation of acid gases at high evaporative concentration yields PHCl ~10^{-7} bar at boiling temperatures, with pH staying >5 in condensation areas.

- Salt separation on the drip shield is not predicted, because the volume of brine that remains once the first salt precipitates (NaCl) is too small to allow further brine movement.

- The clay minerals in the invert neutralize the pH of seepage water, although this result is sensitive to assumptions regarding the kinetics of reactions with clays.

- The drift invert may act as a pH buffer promoting uranophane precipitation and impeding downward migration of radionuclides at elevated concentrations (Figures 2 and 3).

These results are preliminary and specific to the conditions considered. The buffer effects could be different (stronger or weaker) depending on the initial pore water composition and other in-drift physical and chemical conditions.

Related Publications

Zhang, G., N. Spycher, E. Sonnenthal, and C. Steefel, Implementation of a Pitzer activity model into TOUGHREACT for modeling concentrated solutions. Proceedings, TOUGH2 Symposium, Lawrence Berkeley National Laboratory, Berkeley, CA, May 15–17, 2006a.

Zhang, G., N. Spycher, T. Xu, E. Sonnenthal, and C. Steefel, Reactive geochemical transport modeling of concentrated aqueous solutions: Supplement to the TOUCHREACT Users's Guide for the Pitzer ion-interaction model. Report LBNL-62718, Lawrence Berkeley National Laboratory, Berkeley, CA, 2006b.
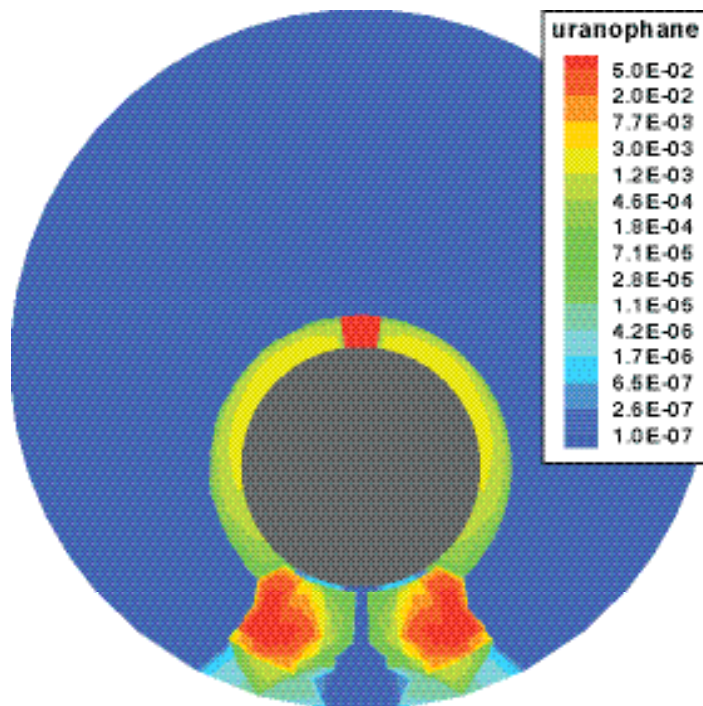

Figure 2. Simulated distribution of uranophane (mol/ m^3 of medium) precipitated after 25 years of continuous dripping. Precipitation of this mineral in the drift invert removes most of the UO_2^{+2} mass from the seepage water and substantially decreases the UO_2^{+2} concentration in water percolating out of the drift.
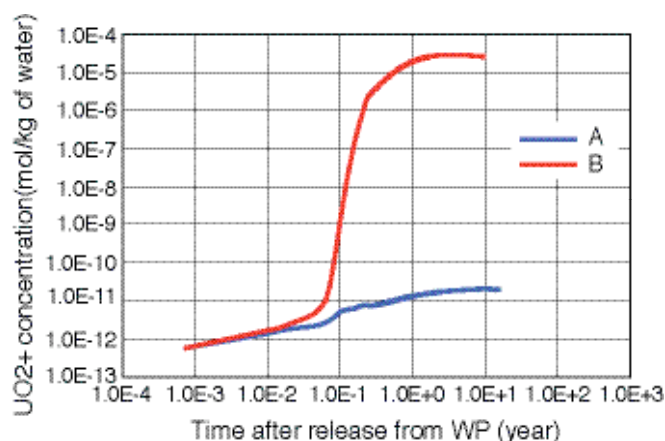

Figure 3. Simulated time evolution of UO_2^{+2} concentration at the base of the drift, with (A) and without (B) consideration of uranophane precipitation, showing the clear effect of precipitation of this mineral in the drift invert.

DRIFT SHADOW

Nature of Drift Shadows at Analogue Sites
Tim Kneafsey, Teamrat A. Ghezzehei, Grace Su, and Paul Cook, Lawrence Berkeley National Laboratory (LBNL), and Brian Marshall, United States Geological Survey (USGS)

Testing the Concept of Drift Shadow
James Paces and Leonid A. Neymark, United States Geological Survey (USGS); Teamrat A. Ghezzehei and Patrick Dobson, Lawrence Berkeley National Laboratory (LBNL)

Testing the Concept of Drift Shadow with X-Ray Absorption Imaging Experiments
Susan J. Altman, Clifford K. Ho, Aleeca Forsberg, and William Peplinski, Sandia National Laboratories (SNL)

This page intentionally left blank.

Nature of Drift Shadows at Analogue Sites

Tim Kneafsey[1], Teamrat A. Ghezzehei[1], Grace Su[1], Paul Cook[1], and Brian Marshall[2]
[1]Lawrence Berkeley National Laboratory (LBNL) | [2]United States Geological Survey (USGS)

Research Objectives

The drift shadow is a region below an underground void (such as a drift) in an unsaturated environment that is sheltered from downward-percolating water. Such a region forms when capillary forces are too weak to immediately draw percolating water into this region. Thus, radionuclide transport directly below a drift would take place primarily by the slow process of diffusion. The presence of a drift shadow below the drifts at the Yucca Mountain repository would significantly enhance the performance of the repository, and could be engineered by mining tunnels above waste emplacement drifts to shadow these drifts. The drift shadow concept has been demonstrated theoretically (Philip et al., 1989) and by numerical simulation (Houseworth et al., 2003); our objective is to collect the field and laboratory data needed to verify the concept.

Approach

Our approach to investigating the drift shadow is to find a field site containing a natural or mined cavity in the unsaturated zone, measure flow-affecting parameters, predict the drift shadow numerically, and use geophysical, hydrologic, and geochemical tools to assess its presence and extent. In our first year of work, we were able to locate a suitable site, the Atlas Mine at the Black Diamond Mines Regional Preserve in Antioch, California. We are now proceeding with the aforementioned measurements, predictions, and assessments.

Accomplishments

In FY2006 and the first two quarters of FY2007, we:

- Formalized an agreement with the site owner allowing our investigation.

- Prepared seven Technical Implementing Procedures (TIPs) to facilitate our investigation.

- Made initial field and laboratory measurements to gain an understanding of site-relevant parameters.

- Designed, constructed, and surveyed a test bed including an active and passive test. Test bed design used site-specific information and numerical simulation. The resulting test bed is composed of 20 boreholes having lengths ranging from 1.5 m to 4 m.

- Collected and preserved core from the 60 m (200 ft) of boreholes.

- Performed gravimetric moisture analyses of 166 core samples and x-ray scanning of all core retrieved.

- Performed two ground-penetrating-radar investigations of water content between boreholes.

- Initiated deployment of water potential sensors in the boreholes.

Additional information on a number of these accomplishments is presented below.

Initial Field and Lab Tests

We conducted two falling-head ring-infiltrometer tests near our test bed and simulated the water level in the ring and responses of the subsurface electrical resistance probes using a 3-D model.

Field Test Design, Construction, Survey, and Preparation

We developed a three-dimensional iTOUGH2 model (5 m wide, 2.5 m deep, and 10 m high) to aid in test design. In the model, with k= 100 mD, a distinct drift shadow began to form in about 100 days, and a fully developed steady-state drift shadow zone required approximately 300 days. Our test bed (Figure 1) encompasses regions surrounding the upper (machinery) and lower (haulage) drifts.

We surveyed borehole locations and directions, drift geometry and orientation, and relation to ground surface, and have begun installation of monitoring equipment, including 92 calibrated gypsum blocks, 20 custom tensiometers (for water potential), and 26 calibrated thermistors.
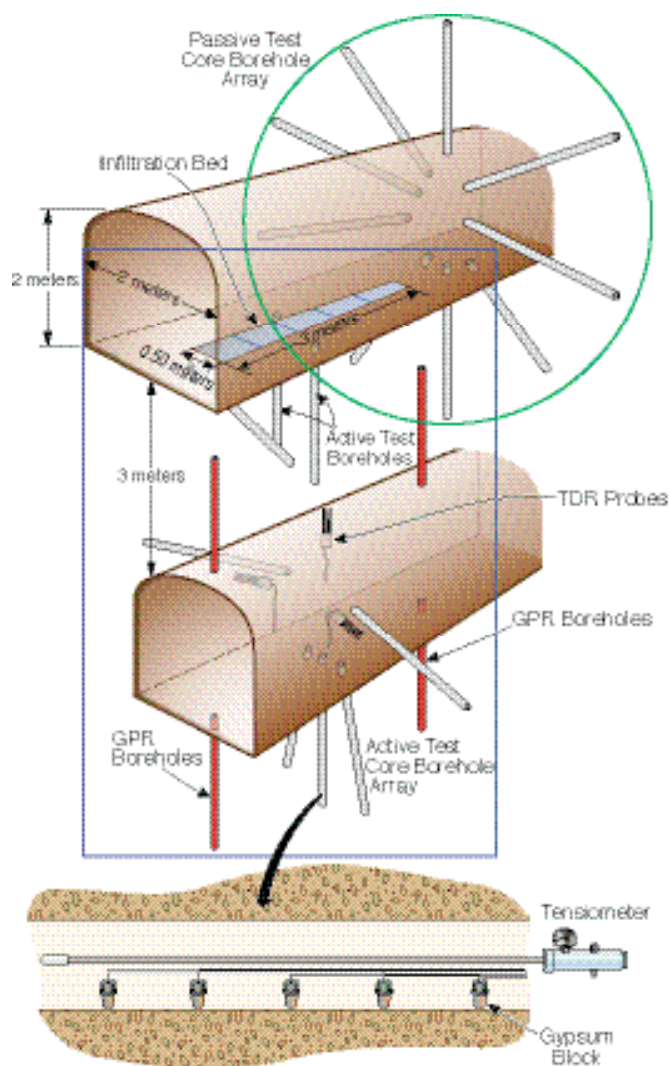
Figure 1. Borehole schematic. Passive test boreholes are identified by the green circle, active test boreholes by the blue box, and ground-penetrating-radar holes by the red boreholes.

Ground Penetrating Radar

We performed two sets of ground-penetrating-radar measurements between adjacent borehole pairs to provide a measure of water content between the boreholes. The region between the two drifts is relatively dry, and water content increases with depth below the lower drift.

Core Collection and Gravimetric Moisture Analysis

We carried out gravimetric moisture analyses of core from each borehole, as well as x-ray scanning of core to identify high-density regions resulting from the deposition of
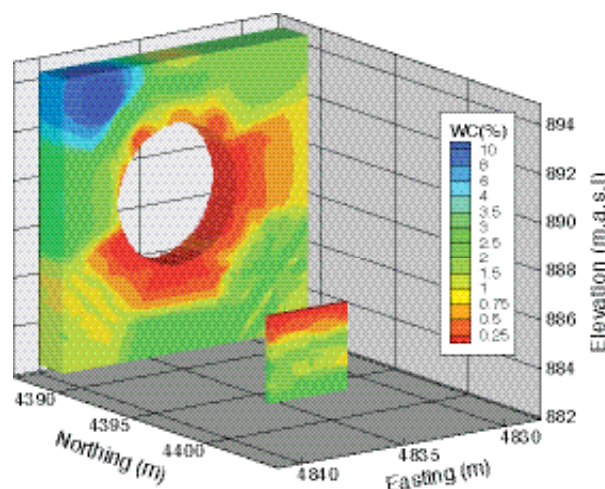

Figure 2. Gravimetric water content (percent) around the upper drift.

evaporite minerals. X-ray scanning provided no indication of a drift shadow. Results of gravimetric moisture analyses of 166 samples from 11 boreholes were interpolated using an inverse-distance approach. The resulting water content distribution around the upper drift is shown in Figure 2.

Dipping, resembling the visible dip of the strata at the site, is clear. The region below the drift is generally drier than the region above; however, water potential (rather than water content) is the preferred parameter to test the presence of drift shadow.

References

Houseworth, J.E., S.A. Finsterle, and G.S. Bodvarsson, Flow and transport in the drift shadow in a dual-continuum model. Journal of Contaminant Hydrology, 62–63, 133–156, 2003.

Philip, J.R., J.H. Knight, and R.T. Waechter, Unsaturated seepage and subterranean holes: Conspectus, and exclusion problem for circular cylindrical cavities. Water Resources Research, 25(1), 16-28, 1989.

Journal Papers Accepted and Conference Papers Given:

Ghezzehei, T.A., T.J. Kneafsey, and G.W. Su, Correspondence of the Gardner and van Genuchten relative permeability functions. Water Resources Research, 2007 (in press).

Su, G.W., T.J. Kneafsey, T.A. Ghezzehei, P.J. Cook, and B.D. Marshall, Field investigation of the drift shadow. Berkeley Lab Report LBNL-59455. Proceedings of the 11th International High-Level Radioactive Waste Management Conference, Las Vegas, NV, April 30–May 4, 2006

Testing the Concept of Drift Shadow

James Paces[1], Leonid Neymark[1], Teamrat Ghezzehei[2], and Patrick Dobson[2]
[1]United States Geological Survey (USGS) | [2]Lawrence Berkeley National Laboratory (LBNL)

Research Objectives

Water percolating through fractured tuff at Yucca Mountain, Nevada, may be diverted around voids in the unsaturated zone (UZ) by capillary forces rather than seeping into openings. Drift shadows, defined as zones of decreased water saturation and flow velocity, may be present for some distance beneath UZ openings until capillary forces reestablish uniform flow. Drift shadows present beneath proposed emplacement drifts may contribute to the performance of the natural-system barrier at the proposed high-level radioactive waste repository, by increasing UZ groundwater travel times. The objective of this project is to study drift shadows beneath natural lithophysal cavities (voids formed during emplacement of tuffs) in the Yucca Mountain UZ that should result in variable degrees of water saturation and differences in chemical and isotopic compositions of whole-rock and pore-water samples.

Approach

To test for the presence of naturally formed drift shadows, uranium (U) concentrations and $^{234}U/^{238}U$ activity ratios (AR) in rock samples were used to evaluate long-term differences in water fluxes. Zones of greater water flux should develop lower U concentrations, because of the high solubility of U in oxidizing, carbonate-rich solutions, and greater depletion of ^{234}U relative to ^{238}U, because of alpha-recoil processes. Therefore, rock samples from drift-shadow zones should have systematic differences in U-series data relative to rock at cavity margins. In addition, drift shadow zones should have pore water with higher concentrations of conservative ions (such as Cl) due to longer residence times and the possibility of greater *in situ* liquid-gas exchange.

Rock samples were collected from lithophysal cavities in the Exploratory Studies Facility (ESF) at 2,979 and 3,018 m from the tunnel portal and in the Enhanced Characterization of the Repository Block (ECRB) Cross Drift at 1,615 and 1,617 m from the ESF. Samples obtained with a ~15 mm diameter percussion drill formed irregular grids beneath each cavity. Hand samples also were collected from the sides and top of two cavities.

Pore-water samples were obtained from five 6 m long dry-cored horizontal boreholes between 1,610 and 1,618 m in the ECRB. Video logs were used to identify lithophysal cavities intersected by these boreholes. Subjacent boreholes angled 3° downward were cored at two of these sites to obtain core 0.3 to 0.5 m beneath cavities intersected in the horizontal holes. Pore water from one of the horizontal boreholes was extracted by ultracentrifugation of 200-gram core samples at ~15,000 revolutions per minute for 6 hours.

Accomplishments

Whole-Rock Analyses:
U-series isotope analyses were completed on 77 whole-rock samples from around lithophysal cavities exposed in tunnel walls. Results show a general covariance between
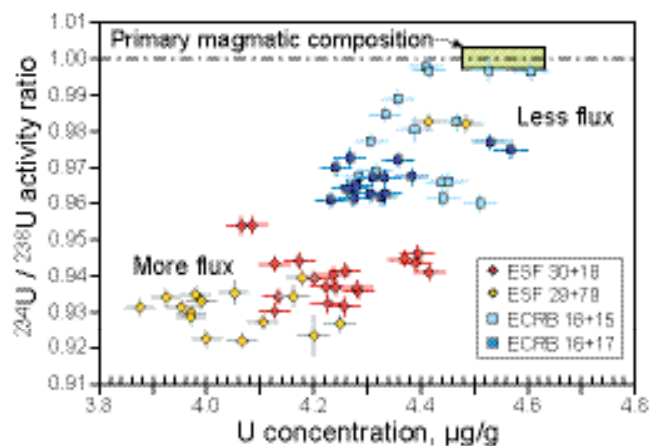

Figure 1. Relations between uranium (U) concentration and $^{234}U/^{238}U$ activity ratio (AR) for whole-rock samples associated with four lithophysal cavities. Error bars represent 2 sigma analytical uncertainties.

rock U concentration and $^{234}U/^{238}U$ AR (Figure 1). Concentrations of other minor and trace elements indicate that the observed trend in U concentrations does not reflect primary magmatic variations. Instead, U-series data are interpreted to reflect greater postdepositional U loss and ^{234}U depletion in samples from the ESF than samples from the ECRB. These results, along with the larger thick-

ness of secondary mineral coatings in the ESF cavities, are interpreted as evidence for greater UZ percolation flux in this area.

Spatial patterns of ^{234}U depletion are present in samples beneath lithophysal cavities. Three of the four cavities have less ^{234}U depletion beneath cavities relative to samples from cavity margins, consistent with the concept of drift shadow. In contrast, results from samples associated with the largest cavity (~130-cm wide) at ESF 3,018 m indicate that more ^{234}U depletion is present beneath the cavity than near its margins. A 3 cm thick secondary mineral coating floors this cavity, which is substantially thicker than coatings in the other cavities, and indicates that it received more water seepage than the other cavities. This finding implies that fluxes exceeded the seepage threshold at this location.

Pore-water Analyses: Gravimetric moisture contents for 22 samples from a 2 m long interval in borehole ECRB DS3 1616 appear correlated with the presence of lithophysal cavities intersected in the borehole, although the geometries of voids intersected by the borehole are difficult to quantify. Pore-water extraction was successful only where moisture contents exceeded 2.5 to 3.0 weight percent. Solute concentration varied with moisture content (highest Cl concentrations are from samples with the lowest moisture contents), implying that evaporation, either in situ or during core drilling, may be an important process controlling pore-water compositions.

Compared to other Yucca Mountain pore-water samples, the samples from borehole ECRB DS3 1616 are more dilute with Cl concentrations between 5.0 and 20.4 mg/L. Weight ratios of NO_3^-/Cl^- between 1.2 and 2.2 are higher than values in other pore-water samples and would have less impact on waste-package corrosion. Concentrations of Cl^-, NO_3^-, and SO_3^{2-} are strongly correlated and are consistent with evaporative concentration by as much as a factor of 4. However, Na^+ and Ca^{2+} concentrations in the same samples vary by less than a factor of 2 and do not regress through zero, indicating that additional processes besides evaporation are involved. Chemical tracers (LiBr) added to the water used for tunnel construction were not detected. These chemical data indicate that (1) both evaporation and water/rock reaction affected pore-water samples, (2) pore-water heterogeneities are maintained at the same spatial scales observed for lithophysae, and (3) moisture contents and concentrations are likely related to the presence of

drift shadows.

Unlike elemental concentrations measured in pore-water samples, uranium and strontium isotope ratios are not affected by evaporative processes. Pore water had $^{234}U/^{238}U$ AR ranging between 1.79 and 2.60, substantially lower than other samples of repository-level pore water and fracture water (calculated from initial $^{234}U/^{238}U$ AR values in fracture minerals). $^{234}U/^{238}U$ AR values do not show clear spatial relations to the large cavity in borehole ECRB DS3 1616, although samples from within the cavity tend to have lower values than samples outside the cavity zone. $^{87}Sr/^{86}Sr$ values determined for five of the pore-water samples ranged from 0.71235 to 0.71259, with no apparent trend with depth in the borehole. These values are within the range observed for other pore-water data from the repository horizon.

Pore water also was extracted from two core samples within the same 2 m long interval by vacuum distillation and analyzed for stable H and O isotopes. Resulting values of -89.5‰δ^2H and -11.9‰$\delta^{18}O$ in one sample and -93.2‰ and -13.1‰ in the other are consistent with infiltration during warmer (Holocene) rather than cooler (Pleistocene) climates. Both samples plot near the global meteoric line, showing no obvious effects of evaporation during drilling.

Modeling: Numerical simulations of drift-shadow dimensions for theoretical matrix- and fracture-flow systems used a two-dimensional dual permeability flow model scaled to dimensions appropriate for the meter-scale lithophysal cavities. Under the gravity-dominated advective fracture-flow conditions present within the proposed repository horizon, preliminary simulations indicate that drift shadows would develop beneath cavities ~1 m in diameter or larger. These simulations only addressed conditions where percolation fluxes do not exceed the seepage threshold into the cavity.

Summary

U-series whole-rock isotope analyses show patterns of disequilibrium that are consistent with conceptual and numerical models of drift shadow associated with cavities in this study. Existing pore-water data associated with lithophysal cavities also support the presence of drift shadows. However, patterns of $^{234}U/^{238}U$ disequilibrium are complicated beneath cavities where percolation fluxes may have exceeded seepage thresholds.

Testing the Concept of Drift Shadow with X-Ray Absorption Imaging Experiments

Susan J. Altman, Clifford K. Ho, Aleeca Forsberg, and William Peplinski
Sandia National Laboratories (SNL)

Research Objectives

X-ray absorption imaging is used to test the concept of the drift shadow in geological samples. The drift shadow model predicts that water travels around underground tunnels, or drifts, leaving areas of high saturation along the sides of the drift (roof-drip lobe) and an area of low saturation beneath the drift (drift shadow). The drift shadow model could impact nuclear waste repositories designed with open tunnels, such as Yucca Mountain, by impacting the flux available to transport waste beneath the repository. However, without strong evidence for the drift shadow effect, it is difficult to justify its inclusion in performance assessment calculations.

Figure 1. Schematic of specimen after sample preparation (A) and in the test cell (B).

Approach

Our study uses x-ray absorption imaging to test the concept of the drift shadow. X-ray absorption imaging techniques have been shown to be a powerful tool to visualize and quantify flow and transport in opaque systems (Altman et al., 2004; Tidwell et al., 2000). Laboratory-scale volcanic tuff samples are imaged to directly visualize pathways of infiltrating water in the vicinity of the drift. In addition, outflow samples are collected in and beneath the model drift to further confirm the visualization results. Through the use of geological samples, we not only test the drift-shadow concept, but also provide data in heterogeneous materials to assist in future numerical modeling.

Samples of Topopah Spring welded tuff (Tsw), collected from Busted Butte, Nevada Test Site, were used for this study. Test cells were prepared with different fracture apertures (Figure 1). Prior to starting an experiment, test cells were saturated with water. At the start of the experiment, a tracer was dripped at a controlled flow rate through four ports at the top of the test cells. Transport through the cell was measured by collecting and weighing sponges both in the drift and at collection ports at the bottom of the flow cell. X-ray images were collected prior to the start of the experiment and at different times during the experiment. By subtracting the image taken prior to the start of the experiment from the images taken during the expe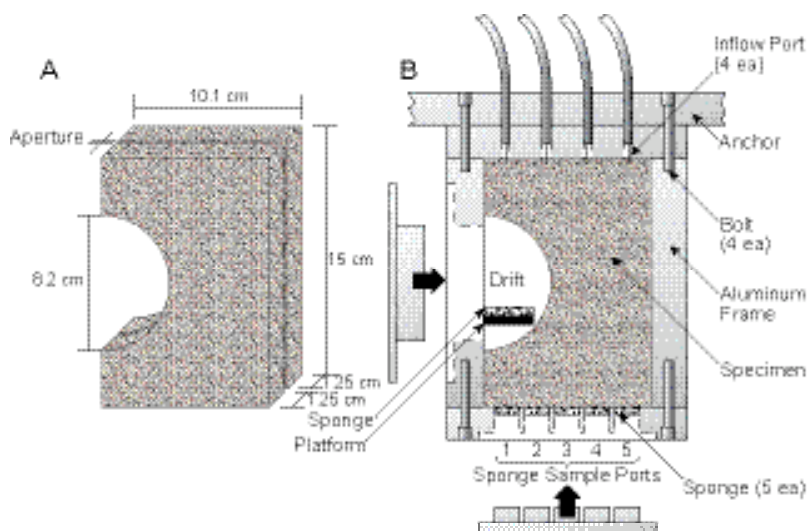riment, the x-ray absorption due to the geological media was removed, and the tracer pathways in the geological samples become visible.

Accomplishments

Experiments were completed by the summer of 2006. Since this time, our focus has been on presenting and publishing our interpretations of the experimental results. Presentations have been made at the Geological Society of America Annual Meeting (October 2005) and the International High-Level Radioactive Waste Management Conference (May 2006). Publications include one in the *Proceedings* for the International High-Level Radioactive Waste Management Conference (Altman et al., 2006) and a manuscript submitted to the *Journal of Hydrology* (Altman et al., in review). A modified version of the conclusions from the *Journal of Hydrology* manuscript is presented below:

X-ray absorption experiments provide clear images of a roof-drip lobe and drift shadow forming in real time on geological samples (Figure 2). The imaging shows a tracer-solution flow path above the drift being diverted around the drift and shedding beyond the drift. In all but two of the tests, less than 1% of the inflow mass was discharged into the drift. The evidence for a drift shadow is generally
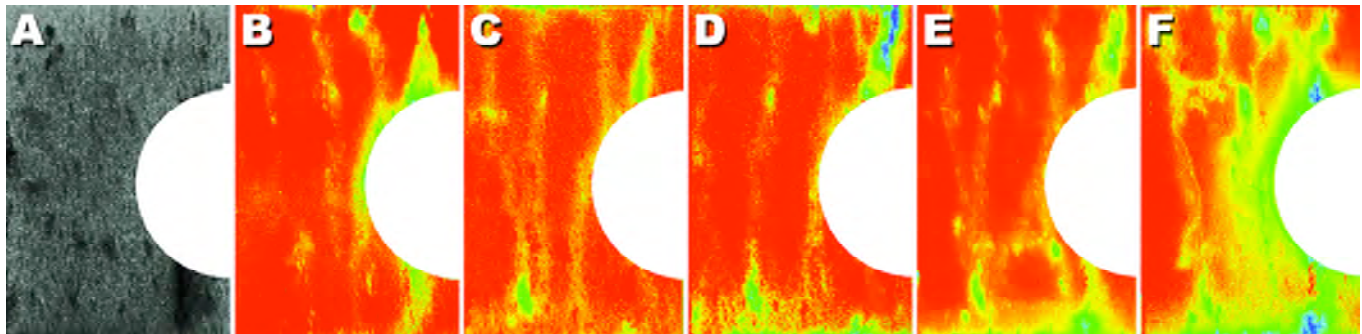
Figure 2. X-ray absorption images of the 250 Ìm aperture test cell taken before (A) and 5 hours (B-F) after the start of experiments. Flow rates are 0.01, 0.05, 0.09, 0.13, and 0.24 mL/min for tests B, C, D, E, and F, respectively. Red going to yellow, green, blue, and purple indicates increasing tracer concentration. Image of cell without tracer (A) shows more porous pumice fragments as darker areas.

demonstrated through the observation of less discharge under the drift and greater discharge just beyond the drift than if flow was uniformly vertical (Figure 3). However, there is also evidence that under the right conditions (low flow rates and small-fracture apertures), water might be transported back under the drift. In addition, natural heterogeneities can influence the extent of the drift shadow effect.

While these studies provide quantitative and visual evidence that only a fraction of the total percolation flux is available for transporting radionuclides immediately beneath the repository, further work is needed to quantify the effect of the drift shadow on radionuclide transport.

The experiments presented here can feed into a numerical modeling exercise that can more fully capture the impact of heterogeneities and the range of hydrogeological parameters (e.g., infiltration rates, fracture apertures). This modeling exercise can also account for the impact of the smaller scale of our experiments relative to field-scale drifts on the experimental results. Thus, these experiments, coupled with future modeling, can provide the data needed for performance assessment calculations to account for the impact of the drift shadow on radionuclide transport. If implemented, such studies could lead to improved natural barrier performance in future calculations.

References

Altman, S. J., A. Forsberg, W. Peplinski, and C. K. Ho, Testing the concept of drift shadow with x-ray absorption imaging. In 2006 International High-Level Radioactive Waste Management, conference held in Las Vegas, NV, April 30–May 4, 2006.

Altman, S.J., A.A. Forsberg, W.J. Peplinski, and C.K. Ho, Experimental observation of the drift-shadow effect using x-ray absorption imaging. J. Hydrol., in review (submitted April 2007).

Altman, S.J., M. Uchida, V.C. Tidwell, C.M. Boney, and B.P. Chambers, Use of x-ray absorption imaging to examine heterogeneous diffusion in fractured crystalline rocks. J. Contam. Hydrol., 69(1–2), 1–26, 2004.

Tidwell, V.C., L.C. Meigs, T. Christian-Frear, and C.M. Boney, Effects of spatially heterogeneous porosity on matrix diffusion as investigated by X-ray absorption imaging. J. Contam. Hydrol., 42(2–4), 285–302, 2000.
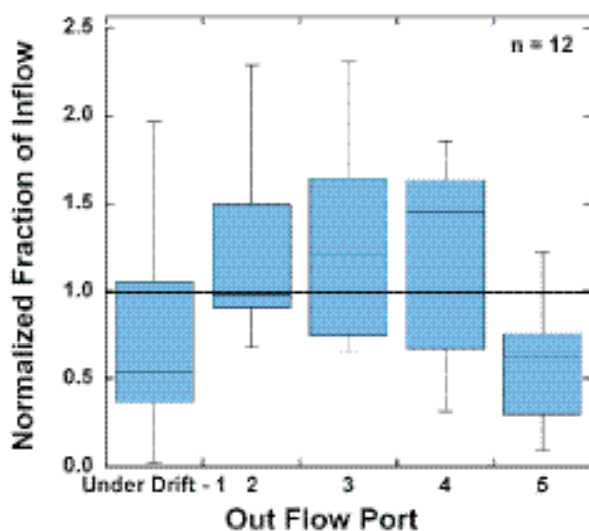
Figure 3. Normalized fraction of inflow discharging through outflow ports for 12 tests presented in Altman et al. (in review). Each box encloses 50% of the values with the central line representing the median value. The bars show the minimum and maximum values. Fractions are normalized such that if the inflow were discharged uniformly, the normalized discharge would be 1.

Office of the Chief Scientist: Research Summaries 2006-2007

UNSATURATED ZONE FLOW AND TRANSPORT

Enhanced Retardation of Radionuclide Transport in Fractured Rock
Hui-Hai Liu, Yinqi Zhang, and Keni Zhang, Lawrence Berkeley National Laboratory (LBNL); Fred J. Molz, Clemson University

Peña Blanca Natural Analogue
Schön S. Levy, Amr Abdel-Fattah, John Dinsmoor, Steve Goldstein, and Michael T. Murrell, Los Alamos National Laboratory (LANL); Paul Cook, Patrick F. Dobson, and Teamrat Ghezzehei, Lawrence Berkeley National Laboratory (LBNL); Mostafa Fayek, University of Tennessee-Knoxville; Philip Goodell and Katrina Pekar, University of Texas-El Paso (UTEP); Richard Ku and Shangde Luo, University of Southern California (USC)

Matrix/Fracture Flow in Subrepository Units
Leonid Neymark and James Paces, US Geological Survey; David Vaniman and Steve Chipera, Los Alamos National Laboratory (LANL)

Pore Connectivity, Episodic Flow, and Unsaturated Diffusion in Fractured Tuff
Qinhong Hu, Lawrence Livermore National Laboratory (LLNL); Robert P. Ewing, Iowa State University; Liviu Tomutsa, Lawrence Berkeley National Laboratory (LBNL)

This page intentionally left blank.

Enhanced Retardation of Radionuclide Transport in Fractured Rock

Hui-Hai Liu[1], Yinqi Zhang[1], Keni Zhang[1], and Fred J. Molz[2]

[1]Lawrence Berkeley National Laboratory (LBNL) | [2]Clemson University

Research Objectives

The matrix diffusion process is crucial for the retardation of contaminant transport in fractured rocks. It has been previously shown that the key parameter controlling the matrix diffusion process, the effective matrix diffusion coefficient, is scale dependent (Liu et al., 2004, Zhou et al., 2006). During FY06/FY07, the focus of our research is on investigating the physical mechanisms behind this scale-dependent behavior.

Approach

Analyses and numerical experiments have been systematically performed to investigate the possible mechanisms behind matrix-diffusion-coefficient scale dependence for some relatively simple fracture-matrix systems. We have identified two possible mechanisms: the flow geometry effect and subsurface heterogeneity effect.

Accomplishments

We have previously investigated how the flow geometry affects the effective matrix diffusion coefficient. According to percolation theory, a flow path consists of both globally connected fractures and relatively small fractures that form local flow loops. A simplified system was constructed that contains a single flow path with different levels of flow loops. This geometry results in a general increase in the effective matrix diffusion coefficient with observation scale. Our conclusion is that a combination of local flow loops and scaling properties in flow-path geometry contributes to the scale dependence of the matrix diffusion coefficient.

During FY06/FY07, we focused on examining how subsurface heterogeneity affects the effective matrix diffusion coefficient. For this purpose, we have developed analytical expressions for the effective matrix diffusion coefficient in two fracture-matrix systems: (1) a single fracture system with a heterogeneous matrix-porosity distribution, and (2) a multiple fracture system with a heterogeneous matrix diffusion coefficient among different fractures.

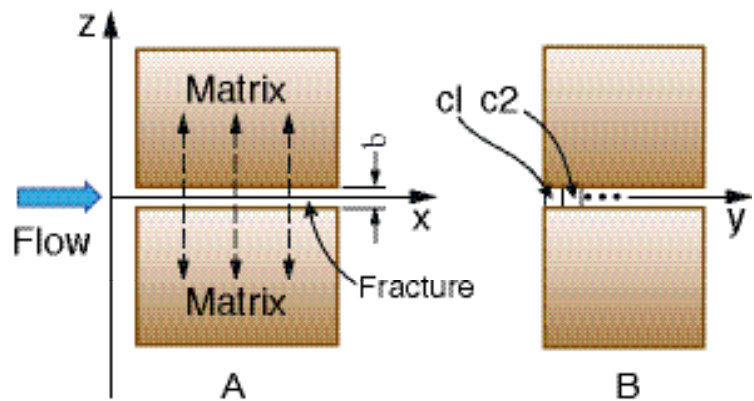In the single-fracture system (Figure 1), we assume matrix

Figure 1. Schematic of a single fracture system.

porosity to be log-normally distributed. Given the intrinsic relation between matrix porosity and matrix permeability (Costa, 2006), the matrix permeability is also log-normally distributed. We derived an analytical formulation (Equation 1) for this system (Liu et al., 2007a):

$$\frac{D_e}{D_m} = \left[\frac{K_e}{K_g} \right]^{\frac{9}{2m^2}} \tag{1}$$

where D_e is the effective matrix diffusion coefficient, K_e is the effective matrix permeability, D_m is the local-scale matrix diffusion coefficient, and K_g is the geometric mean of matrix permeability. For a typical value of $m = 3$ (Costa, 2006):

$$\frac{D_e}{D_m} = \left[\frac{K_e}{K_g} \right]^{\frac{1}{2}} \tag{2}$$

Equation (2) provides an intrinsic relationship between the effective matrix diffusion and the effective matrix permeability. While it has been widely recognized that the effective permeability generally increases with test scale, Equation (2) indicates that the effective matrix diffusion coefficient should follow the same trend as the permeability.

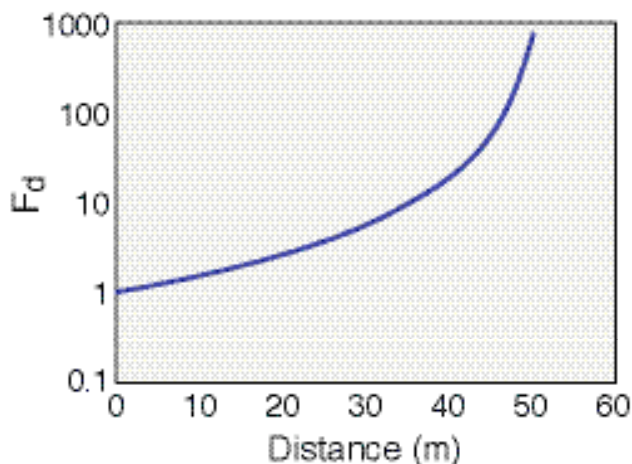In addition to the single fracture system, we also investi-

Figure 2. Effective matrix diffusion coefficient as a function of travel distance.

property values. Obviously, F_d is scale dependent and increases with solute travel distance.

In summary, we have theoretically demonstrated that in addition to effects of flow-path geometry (Liu et al., 2007b), the heterogeneities of rock matrix properties within a single fracture and among different flow channels also contribute to the scale dependence of the effective matrix diffusion coefficient.

References and Journal Articles

Costa, A., Permeability-porosity relationship: A reexamination of the Kozeny-Carman equation based on a fractal pore-space geometry assumption. Geophy. Res. Lett., 33, L02318, doi:10.1029/2005GL025134, 2006.

Liu, H.H., G.S. Bodvarsson, and G. Zhang, The scale-dependency of the effective matrix diffusion coefficient. Vadose Zone Journal, 3, 312–315, 2004.

Liu, H.H., Y. Zhang, and F.J. Molz, Scale dependence of the effective matrix diffusion coefficient: Some analytical results. Vadose Zone Journal (in press), 2007a.

Liu, H.H., Y. Zhang, Q. Zhou and F.J. Molz, An interpretation of the potential scale dependence of effective matrix diffusion coefficient. Journal of Contaminant Hydrology, 90(1–2), 41–57, 2007b.

Neretnieks, I., A stochastic multi-channel model for solute transport—Analysis of tracer tests in fractured rock. J. Contam. Hydrol., 55, 175–211, 2002.

Tsang, C.F., and I. Neretnieks, Flow channeling in heterogeneous fractured rock. Review of Geophysics, 36(2), 1998.

Zhou, Q, H.H. Liu, F.J. Molz, Y. Zhang and G.S. Bodvarsson, Effective matrix diffusion coefficient for fractured rock: Results from literature survey. Journal of Contaminant Hydrology (in press), 2006.

gated matrix diffusion in a more realistic multiple-fracture system. Flow and transport processes in such a system are generally characterized by flow channels (e.g., Tsang and Neretnieks, 1998). Different flow channels may have different flow and transport properties. In this study, we use a simplified conceptual flow model to investigate the effects of interchannel heterogeneity on diffusive properties. Specifically, we consider a simplified multichannel system in which each flow channel has uniform properties and does not mix with any other channels, except at influent and effluent points. Similar conceptual models have been used by other researchers to analyze flow and transport processes in fractured rock (e.g., Neretnieks, 2002). These channels have the same length, width, fracture aperture, and water velocity, but different matrix diffusion coefficients. This treatment allows us to exclude the effects of dispersion processes and focus on the effects of variability in diffusive properties among different flow channels.

Based on the above conceptual model and simplifications, an analytical solution was derived for the ratio of effective matrix diffusion coefficient to the averaged local-scale diffusion coefficient, F_d, for a multiple fracture system. Figure 2 shows F_d as a function of test scale for some typical rock

Peña Blanca Natural Analogue

Schön S. Levy[1], Amr Abdel-Fattah[1], Paul Cook[2], John Dinsmoor[1], Patrick F. Dobson[2], Mostafa Fayek[3], Teamrat Ghezzehei[2], Steve Goldstein[1], Philip Goodell[4], Richard Ku[5], Shangde Luo[5], Michael T. Murrell[1], and Katrina Pekar[4]

[1]Los Alamos National Laboratory (LANL) | [2]Lawrence Berkeley National Laboratory (LBNL)
[3]University of Tennessee-Knoxville | [4]University of Texas-El Paso (UTEP) | [5]University of Southern California (USC)

Research Objectives

The objective is to study radionuclide transport at a site with characteristics analogous to a nuclear-waste repository at Yucca Mountain, and to use the results to test an entire process model and total system performance assessment. This will be accomplished by using field and laboratory measurements and process-model results from the Peña Blanca, Chihuahua, México, site. A three-dimensional conceptual and numerical model of radionuclide transport in the unsaturated and saturated zones will be developed.

Specific objectives for improved understanding include (1) identifying active fractures and the extent of fracture-matrix geochemical interaction, (2) investigating aqueous transport behavior in the unsaturated and saturated zones, (3) studying the role of colloid transport and colloid-facilitated transport of radionuclides; and (4) studying surficial and shallow subsurface transport processes.

Approach

The Peña Blanca Nopal I site, in Chihuahua, México, is a former mine in a uranium ore body within fractured, welded tuff similar to the repository host rock at Yucca Mountain. The site is in the southern Basin and Range province in an arid environment with a thick (>200 m) unsaturated zone. Three wells were drilled within and adjacent to the ore body, providing access to saturated-zone waters. A seepage-collection system in an old mine adit provides information about percolating water in the unsaturated zone. Field work also includes core sampling, sampling of fractured rock at various distances from the ore body, and mapping, sampling, and *in situ* gamma surveying of surficial materials related to previous surface storage of high-grade ore. Structural and stratigraphic studies provide a basis for the assembly and analysis of geochemical data. Field data, plus chemical and isotopic analysis of rock and water samples, provide the input for process models and a total-system performance assessment.

Accomplishments

Research results were presented at the 2005 Geological Society of America Annual Meeting, the 2006 International High-Level Radioactive Waste Management Conference, and the 2007 American Geophysical Union Joint Assembly.

Site visits conducted throughout 2006 concluded in December 2006. Saturated-zone waters were collected by bailing or pumping on-site wells and by sampling near-site wells being pumped for agricultural use. In August 2006, downhole instruments to monitor water level, pH, and dissolved oxygen were installed in the three onsite wells. The recorded data were downloaded periodically by Autonomous University of Chihuahua faculty and students, who will analyze the data. Large-volume pumped-water samples were run through manganese cartridge filters to collect short-lived radionuclides. Samples were also collected for colloid and radon analysis.

Water samples were collected from a seepage-collection array in an adit. Seepage water collection involved using fixed bottles with collector funnels and automated columns that recorded volume and time of seepage water arrival. A weather station installed in March 2006 recorded continuous measurements of basic meteorological data. Figure 1 shows rainfall and seepage volumes at the automated collectors between May 2006 and December 2006.
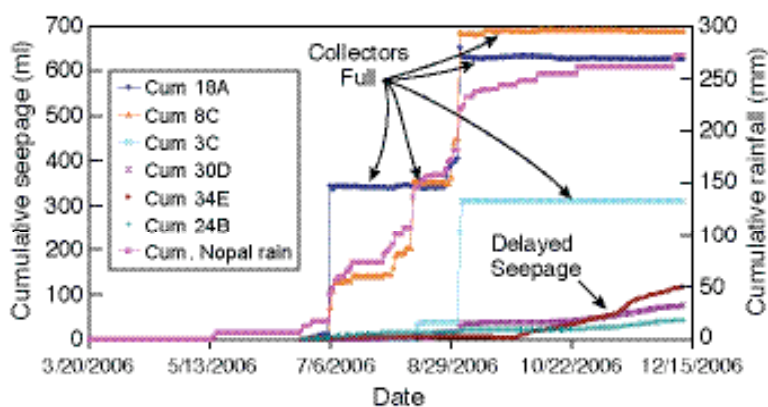

Figure 1. Rainfall and seepage water collected using automated columns at Nopal I (arrows indicate the maximum volume of water in the automated seepage collectors).

The first big storm of the summer rainy season was in July. Data show that in two of the collection sites, seepage water traveled through 8 m of fractured tuff within two hours (the measurement interval) or less. Seepage arrival at the other collectors was much more gradual. These results clearly demonstrate the existence of fast and slow flow pathways.

Seepage waters are enriched in deuterium (D) and ^{18}O relative to saturated-zone waters. A subset of the oxygen isotope data, representing seepage waters from automated columns at 18A and 27C, is shown in Figure 2 as a function of time. There is a marked temporal variation in composition related to the timing of the seasonal rainy period. Both δD and $\delta^{18}O$ values increase as the dry season progresses, and then a sharp decrease in values occurs right after the onset of the summer monsoon season (first week of July). The increase in δD and $\delta^{18}O$ values during the dry season is likely a result of evaporation occurring as water slowly infiltrates through the rock mass.
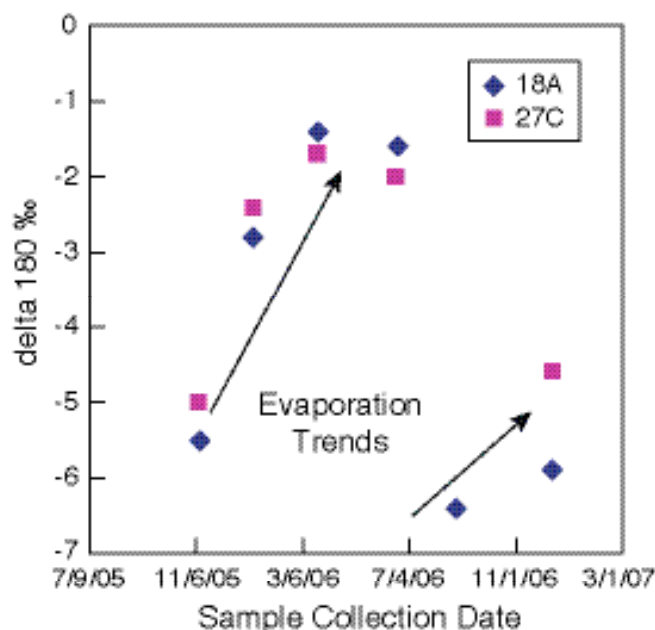

Figure 2. Oxygen isotopic data for seepage waters from two automated collectors at Nopal I.

In general, there are high U concentrations and low $^{234}U/^{238}U$ ratios (close to secular equilibrium) in waters from the front of the adit and low U concentrations with high $^{234}U/^{238}U$ values in samples from the rear of the adit. These results confirm the concept that water from the front of the adit has experienced a longer rock-water interaction time and/or greater U dissolution rate relative to waters

from the rear of the adit. The larger data set shows no seasonal variation of uranium isotopic systematics.

Analyses of ultra-filtered well waters collected in 2006 indicate that ~93–97% of the uranium present is truly dissolved and not in colloidal form. Particle counts for local and regional well samples collected in 2004–2006 indicate colloid contents ranging from 1.0E8 to 1.4E6 particles/mL (~0.2 to 0.003 mg/L). Particle counts for the Nopal I wells have decreased from 2004 to 2006; the earlier, higher counts may have been related to drilling operations. There is a bimodal distribution of colloid surface charge (one population negatively charged and one population neutral or slightly positive) that may reflect the presence of both natural and anthropogenic (e.g., bacteria) colloids.

Uranium concentrations for well waters collected in August 2006 are approaching "steady-state" or "equilibrium" concentrations (23 ppb in PB-1 and 398 ppb in PB-3; Figure 3), down from values as high as 18,000 ppb soon after the wells were drilled. The rates of decrease in aqueous uranium concentration since the wells were drilled (in 2003) suggest that groundwater flow rates are <10 m/yr.
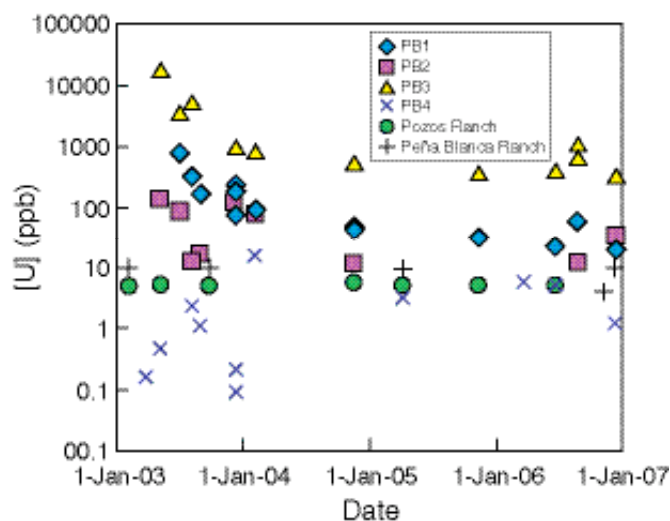

Figure 3. Time series for uranium concentrations in saturated-zone waters of the Peña Blanca region.

A study of ^{238}U-^{239}Pu disequilibrium in four saturated zone water samples (PB1, PB2, PB3, and PB4) collected in December 2003 was completed. All samples had $^{239}Pu < 50$ atoms/g, and sample PB3 had the highest U concentration of 966 ppb. These values were used to calculate an upper limit Pu/U ratio of 2E-14, based on the assumption that any Pu in the sample is derived from neutron reactions

with ^{238}U. Comparison of this value with the lower-limit secular equilibrium ratio of 2E-12 allows us to estimate that R(Pu)/R(U) is at least ~100, where R is the retardation factor (transport rate of groundwater/transport rate of radionuclide). This means that Pu is at least two orders of magnitude less mobile than U in the saturated zone at Nopal I.

Prior studies of ^{238}U-^{234}U-^{230}Th-^{226}Ra disequilibria showed that R(Ra)/R(U) ranges from 0.01 to 100, and R(Th)/R(U) ranges from 1 to 200. Efforts to determine R(U) from short-lived nuclide data are under way, but it typically is on the order of ~1,000 elsewhere. The short-lived nuclide data were used to calculate retardation factors on the order of 1,000 for radium and 10,000 to 10,000,000 for lead and polonium. Radium has enhanced mobility in adit water and fractures near the uranium deposit. Mean fracture width in the area is estimated to vary from ~0.2 to ~4.0 μm. Also, well-water samples were sent to the DOE Idaho Falls laboratory for analysis of technetium-99, but all samples were below the detection limit of about E-6 ppb for concentrated samples.

Preliminary mineral isotopic ages from Nopal I suggest the following: (1) a uraninite mineralizing event at 32±8 Ma, possibly related to Basin and Range tectonism; (2) an oxidizing event at ~3.1 Ma that formed uranophane; (3) a second uraninite mineralizing event at ~1.6 Ma; and (4) subsequent oxidizing events that precipitated schoepite (~85 ka) and weeksite/boltwoodite (~41 ka). The relation between <1 Ma uraninite from the Pozos conglomerate 100 m below the main ore body and the ~1.6 Ma uraninite is unclear. However, the conglomerate may have scavenged uranium moving downward through the unsaturated zone.

Forty-element chemical analyses were obtained for 20 Peña Blanca samples, including high-grade ore and host rock. These analyses will provide source-term information for numerical modeling of radionuclide transport. Gamma-ray spectroscopy of soils beneath and downslope of a block of high-grade uranium ore, emplaced on the ground surface during active mining, indicates that dispersion of particulates from the ore into the soil has reached a depth of 20 cm over 25 years. A preliminary effort has been made to calculate effective dispersion coefficients for ^{234}Th, ^{230}Th, ^{234}U, ^{226}Ra, and ^{210}Pb in the soil.

Related Publications

Presentations made at the GSA annual meeting in October 2005 were listed in the *OSTI Annual Report 2005*.

Fayek, M., M. Ren, P. Goodell, P. Dobson, A. Saucedo, A. Kelts, S. Utsunomiya, R. Ewing, L. Riciputi, and I. Reyes, Paragenesis and geochronology of the Nopal I uranium deposit, Mexico. Proceedings of the 11th International High-Level Radioactive Waste Management Conference, pp. 55–62, Las Vegas, Nevada, April 30–May 4, 2006.

French, D., E. Anthony, and P. Goodell, U-Series disequilibria in soils, Peña Blanca Natural Analogue, Chihuahua, Mexico. Proceedings of the 11th International High-Level Radioactive Waste Management Conference, pp. 63–69, Las Vegas, Nevada, April 30–May 4, 2006.

Ghezzehei, T., P. Dobson, J. Rodriguez and P. Cook, Infiltration and seepage through fractured welded tuff. Proceedings of the 11th International High-Level Radioactive Waste Management Conference, pp. 105–110, Las Vegas, Nevada, April 30–May 4, 2006.

Goldstein, S.J., S. Luo, T. Ku, and M. Murrell, Uranium-series constraints on radionuclide transport and groundwater flow at the Nopal I uranium deposit, Sierra Peña Blanca, Mexico. Proceedings of the 11th International High-Level Radioactive Waste Management Conference, pp. 215–222, Las Vegas, Nevada, April 30–May 4, 2006..

Luo, S., T. Ku, V. Todd, M. Murrell, and J. Dinsmoor, Increased concentrations of short-lived decay-series radionuclides in groundwaters underneath the Nopal I uranium deposit at Peña Blanca, México. Eos Transactions, American Geophysical Union, 88 (23), Joint Assembly Supplement, Abstract GS22A-03, 2007.

Pekar, K., P. Goodell, J. Walton, E. Anthony, M. Ren, Modeling of U-series radionuclide transport through soil at Peña Blanca, Chihuahua, México. Eos Transactions, American Geophysical Union, 88 (23), Joint Assembly Supplement, Abstract GS22A-02.

Saulnier, G., The Peña Blanca Natural Analogue performance assessment model. Proceedings of the 11th International High-Level Radioactive Waste Management Conference, April 30-May 4, 2006, Las Vegas, Nevada, 228-235, 2006.

This page intentionally left blank.

Matrix/Fracture Flow in Subrepository Units

Leonid Neymark[1], James Paces[1], David Vaniman[2], and Steve Chipera[2]

[1]US Geological Survey | [2]Los Alamos National Laboratory (LANL)

Research Objectives

The objective of this study is to investigate the time-integrated fracture-matrix interaction and transport of natural uranium (U) in zeolitized tuffs below the proposed repository at Yucca Mountain, Nevada, by comparing the mineralogical, chemical, and U-series isotopic compositions of samples from fracture surfaces and from variably fractured rocks.

Approach

Retardation of radionuclides by sorption on minerals in the rocks along downgradient groundwater flow paths is a positive attribute of the natural barrier at Yucca Mountain, Nevada, the site of a proposed high-level nuclear waste repository. Alteration of volcanic glass in nonwelded tuffs beneath the proposed repository horizon produced thick, widespread zones of zeolite- and clay-rich rocks with high sorptive capacities. The high sorptive capacity of these rocks is enhanced by the large surface area of tabular to fibrous mineral forms, which is about 10 times larger in zeolitic tuffs than in devitrified tuffs, and about 30 times larger than in vitric tuffs. The alteration of glass to zeolites, however, was accompanied by expansion that reduced the matrix porosity and permeability. Because water would then flow mainly through fractures, the overall effectiveness of radionuclide retardation in the zeolitized matrix actually may be decreased relative to unaltered vitric tuff.

Isotope ratios in the decay chain of ^{238}U are sensitive indicators of long-term water-rock interaction. In systems older than about 1 m.y. that remain closed to mass transfer, decay products of ^{238}U are in secular radioactive equilibrium where $^{234}U/^{238}U$ activity ratios (AR) are unity. However, water-rock interaction along flow paths may result in radioactive disequilibrium in both the water and the rock, the degree of which depends on water flux, rock dissolution rates, α recoil processes, adsorption and desorption, and the precipitation of secondary minerals.

The effects of long-term water-rock interaction that may cause radionuclide retardation were measured in samples of Miocene-age subrepository zeolitized tuffs of the Calico Hills Formation (Tac) and the Prow Pass Tuff (Tcp), from borehole USW SD-9 (Engstrom and Rautman, 1996) near the northern part of the proposed repository area. Mineral abundances and whole rock chemical and U-series isotopic compositions were measured in unfractured core samples (depth interval 451.1 to 633.7 m) representing rock matrix, in rubble (about 1 cm) rock fragments representing zones of higher permeability (assuming that the rubble core indicates a broken zone in the rock mass rather than an artifact of drilling), and in samples from surfaces of natural fractures representing potential fracture pathways. U concentrations and isotopic compositions also were measured in samples of pore water obtained by ultracentrifugation or by leaching rock samples with deionized H_2O. The concentrations and isotopic compositions of loosely bound U adsorbed on reactive mineral surfaces were obtained by analyzing 1 M sodium acetate (NaOAc) leachates of whole-rock samples.

Mineral abundances were measured at Los Alamos National Laboratory by x-ray powder diffraction methods using the full-pattern quantitative analysis program FULL-PAT. Chemical compositions of major and trace elements were determined at the U.S. Geological Survey (USGS) laboratory in Denver by several techniques, including standard x-ray fluorescence spectroscopy (XRF) and inductively coupled plasma-mass spectrometry (ICP MS) techniques. Uranium concentrations and isotopic compositions were measured at USGS using a thermal ionization mass spectrometer (TIMS). Reproducibility of TIMS analyses was about 1% (2σ) for elemental concentrations and 0.2% for U isotope ratios. Atomic isotope ratios were converted to activity ratios using known decay constants.

Accomplishments

The most common secondary minerals in 35 samples of the zeolitized tuff are clinoptilolite (0.5 to 76.3 %), opal-CT (6.5 to 21.8 %), mordenite (1.2 to 22.4 %), and smectite (0.1 to 44 %). Fracture surfaces have more smectite (median value of 6.1%) than unfractured and rubble core (median value of 3.2%).

Concentration trends with depth for whole-rock samples from the upper 50 m of the Tac indicate accumulation of Ca accommodated by loss of Na as a result of downward water movement and cation exchange within the zeolitized rock sequence, consistent with published results

(Vaniman et al., 2001). However, systematic variations with depth and zeolite abundance are not observed for U concentrations over this same depth interval.

Uranium contents in NaOAc leachates (0.012 to 0.071 µg/g rock) represent a mobile U component adsorbed on mineral surfaces or in readily acid-soluble secondary minerals. Compared with whole-rock analyses, these data indicate that the adsorbed U comprises 0.3 to 1.7 percent of total rock ^{238}U. These data allow estimates of the time-integrated *in situ* U partition coefficient ($K_d=C_s/C_w$, where C_s and C_w are concentrations in the solid and water, respectively) under natural flow conditions. Use of median U concentrations in pore water (5 ng/mL) and NaOAc leachates (0.035 µg/g rock) yields an estimate of the ^{238}U K_d value of about 7 mL/g. This value is larger than the value of 0.5 mL/g obtained for crushed tuffs from laboratory batch experiments that currently is used for zeolitized units at Yucca Mountain (BSC, 2004, Table 5-1).

Whole-rock samples of unfractured core, rubble core, and fracture surfaces have similar ^{234}U/^{238}U AR, ranging from 0.92 to 1.16 indicating both enrichments (^{234}U/^{238}U AR>1) and depletions (^{234}U/^{238}U AR<1) in the daughter ^{234}U relative to the parent ^{238}U. In contrast to the rock samples, all pore water and rock leachate samples have elevated ^{234}U/^{238}U AR ranging from 1.1 to 5.2. Whole-rock ^{234}U/^{238}U AR greater than 1 for these zeolitized rocks contrast with data from samples of the welded part of the Topopah Spring Tuff (Tpt), the proposed repository horizon, that invariably have ^{234}U/^{238}U AR <1. The depletion in ^{234}U in Tpt rocks is caused by preferential removal of ^{234}U by the percolating water as a result of α recoil processes. Therefore, the large ^{234}U/^{238}U AR in pore water and in U sorbed on mineral surfaces indicate that ^{234}U removed from overlying units is transported in percolating water and retained in underlying zeolitized units. U-series isotope data for whole-rock samples from subrepository units having ^{234}U/^{238}U AR > 1 also strongly support the potential for retention of U from percolating water by zeolitized rocks and indicate that amounts of retardation of radionuclides may be greater than currently credited to zeolitized rocks at Yucca Mountain.

Evolution of ^{234}U/^{238}U AR in zeolitized rocks continuously adsorbing U from percolating water is described by a simple box model. The model assumes that U in zeolitized rock is derived from three components: (1) U in the rock matrix; (2) U adsorbed onto mineral surfaces from percolating water; and (3) ^{234}U produced from decay of adsorbed ^{238}U and implanted into the rock matrix by alpha-recoil processes. The model does not consider U loss or gain from the relatively slower processes of bulk rock dissolution and secondary mineral precipitation. According to simulations from this model, the observed similarity of ARs in samples of pore water and NaOAc rock leachates indicates that U adsorption in zeolitized tuffs from percolating water is a reversible process occurring at rates much faster than radioactive decay of ^{234}U. Values of time-integrated *in situ* distribution coefficients $K_d \gg 1$ for U adsorption indicate that zeolitized rocks may be important in retardation of U and other actinides with similar geochemical properties in the subrepository zeolitized units in the Yucca Mountain UZ. The *in situ* retardation factor for U in samples of zeolitized rocks is as much as 290, which means that U moves through zeolitized rocks much more slowly than the percolating water.

References

BSC, Technical Basis Document No. 10: Unsaturated zone transport, Revision 1. Bechtel SAIC Company, LLC, Las Vegas, Nevada. Accessed March 6, 2006, at http://www.lsnnet.gov (LSN# NRC000024904), 2004.

Engstrom, D.A. and C.A. Rautman, Geology of the USW SD 9 Drill Hole, Yucca Mountain, Nevada," SAND96-2030, 128 p., Sandia National Laboratories, Albuquerque, New Mexico. Accessed March 6, 2006, at http://www.lsnnet.gov (LSN# DEN000707221), 1996.

Vaniman, D.T., S.J. Chipera, D.L. Bish, J.W. Carey, and S.S. Levy, Quantification of unsaturated-zone alteration and cation exchange in zeolitized tuffs at Yucca Mountain, Nevada, USA. Geochimica et Cosmochimica Acta, 65, 3409–3433, 2001.

Pore Connectivity, Episodic Flow, and Unsaturated Diffusion in Fractured Tuff

Qinhong Hu[1], Robert P. Ewing[2], and Liviu Tomutsa[3]

[1]Lawrence Livermore National Laboratory (LLNL) | [2]Iowa State University | [3]Lawrence Berkeley National Laboratory (LBNL)

Research Objectives

In low-permeability, unsaturated fractured rock, water flows predominantly through the interconnected fracture network, with some water moving into or out from the neighboring matrix rock. During flow episodes, wetting advectively transports radionuclides from fractures into the matrix; between flow episodes, drying at the fracture face advectively moves radionuclides back toward the fracture. Diffusion transports radionuclides from the fracture into the matrix (matrix diffusion), or from the matrix back into flowing fractures (back diffusion). Finally, some radionuclides in the matrix sorb onto matrix rock. These fracture-matrix interactions—with interacting wetting and drying, diffusion, and sorption—tend to retard breakthrough of a radionuclide pulse released to the fracture network. Factors such as matrix pore connectivity, and the timing and magnitude of fracture flow events, influence these interacting processes. These factors are investigated in our work.

Approach

We have developed and used innovative approaches (e.g., application of imbibition tests to probe pore connectivity) and techniques (e.g., the unsaturated transport-sorption method, laser ablation coupled with inductively coupled plasma-mass spectrometry [LA/ICP-MS] for microscale solid sampling). Coupled with pore-scale network modeling, these approaches and techniques are used to further understand and quantify the interacting imbibition-diffusion-sorption processes influencing radionuclide transport in unsaturated fractured rock at Yucca Mountain.

Accomplishments

Preparation of Initially Moist Samples

Partially saturated cores were obtained by equilibrating initially fully saturated cores within relative humidity (RH) chambers controlled by different oversaturated brines until they reached constant weights. Two RH chambers, with respective RH values of 44% (mimicking the low RH during the heat-dissipation phase after nuclear waste package emplacement) and 98% (mimicking the in situ condition of the vadose zone at Yucca Mountain), were used in this project. Equilibrated core samples were then used in the tests for tracer imbibition and unsaturated diffusion.

Unsaturated Transport-Sorption Tests

Unsaturated transport-sorption tests were performed on TSw, CHv, and CHz samples, imbibing a tracer solution into samples at different antecedent water saturations (oven-dried, equilibrated at 44% or 98% RH). The tracer solution contained a suite of nonsorbing and sorbing tracers (including ReO_4^-, and the radionuclides ^{237}Np and ^{242}Pu). We then used LA/ICP-MS to measure the fine-scale distribution of tracers as a function of distance from the imbibing rock face. Figure 1 shows the nonretarded transport of ReO_4^- and transport delayed by sorption for ^{237}Np and ^{242}Pu tracers in TSw34 samples at different antecedent water saturations. For imbibition into an initially dry core, the ReO_4^- front is steep, because a strong capillary force drives advective flow and tracer transport (Figure 1a). During imbibition into a moist medium, solutes disperse by mixing with "old" water, and thus a less sharp ReO_4^- profile is observed (Figure 1c).

Saturated and Unsaturated Tracer Diffusion

Saturated diffusion tests were conducted to investigate tracer diffusion into fully water-saturated cylindrical rock samples (TSw34, CHv, and CHz). We directly mapped the tracer concentration distribution in the rock sample after a certain diffusion time, which ranged from minutes to one day, depending upon rock properties.

Following our published two-element (source-sink) approach (Hu et al., 2004), we conducted unsaturated diffusion tests for three tuff samples under two initial water saturations (44 and 98% RH equilibrated). Tracer distributions on the surface, as well as in the interior, of both elements were immediately mapped using LA/ICP–MS. Analysis to obtain the diffusion coefficient is under way. Preliminary results show the expected diffusion at high water saturation, while diffusion at lower (initially equilibrated at 44% RH) is significantly hindered.
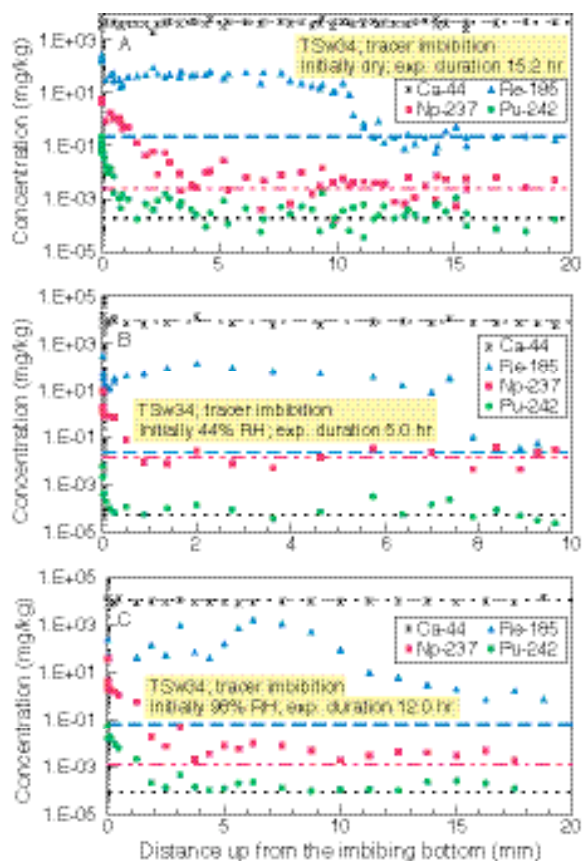
Figure 1. Distribution of imbibed tracers in initially (A) dry, (B) moist at 44% RH, and (C) moist at 98% RH TSw34 cores. Ca concentration intrinsic to the rocks is distributed uniformly. Dashed lines are background levels for each tracer.

Episodic Fracture Flow and Tracer Transport

We have conducted the fracture flow test with the TSw34 devitrified rock under episodic flow events. We prepared a saw-cut fracture core (length 10.2 cm, diameter 4.4 cm, and fracture aperture 100 µm) for TSw34 initially equilibrated at >97% relative humidity. Episodic flow involved four cycles of tracer solution flow within the fracture, followed by flushing with high humidity air. Each flow episode contained at least one nonsorbing tracer (^3H, Se, Br, Mo, ^{99}Tc, I, and Re) and one sorbing tracer (Sr, Cs, ^{235}U, ^{237}Np, and ^{241}Pu). The nonsorbing ^3H and ReO_4^- serve as diffusivity tracers with different aqueous diffusion coefficients.

Liquid effluent from the flow reactor was analyzed to obtain the breakthrough curves of non- or less-retarded tracers. After the flow tests were complete, the flow reactor was opened and the distribution of strongly retarded tracers within the fractured core characterized by LA/ICP-MS.

Results indicate interacting imbibition, diffusion, and sorption, which will contribute to radionuclide retardation under fracture-dominated preferential flow.

Pore-Scale Network Modeling

Some of the laboratory imbibition tests showed two distinct regimes, having slopes of one-half and one-quarter in log-log (cumulative mass imbibed over time) space. "Normal" imbibition gives the slope of one-half (the imbibition front moves with the square root of time), but the lower-slope regime appears in rock with poorly interconnected pore space. In some cases, imbibition transitioned from low-slope to normal-slope behavior; the opposite was never observed. This behavior was produced in the pore-scale simulations as well, with bonds in the cubic lattice pruned almost to the percolation threshold. It is known from percolation theory that processes operating at scales smaller than the correlation length will exhibit anomalous behavior, while above that scale they will behave normally. The distance from the inlet face at which the slopes cross from anomalous to normal is the correlation length of percolation theory and is related to the connectedness of the medium.

The measured crossover distance is a function of both pore connectivity and sample size and shape. This past year, we ran multiple simulations of different-shaped lattices, with length:diameter ratios ranging from 1/8 to 8. These were run at several connectivity values above the percolation threshold. To cope with the high variance of samples near the percolation threshold, we ran several hundred additional simulations at and just above the threshold itself. Simulations were slower the closer they were to the percolation threshold, so significant computer time was involved in these studies.

The statistics of the imbibition curves, whether measured or simulated, pose some challenges. How should the breakpoint (where a curve changes slope) be determined, especially when the data are noisy or the break appears gradual? How should we decide whether a given curve is "really" one line, or two? One new method—the Weighted Hidden Markov Method—and the classical 3-parameter minimum sum of squares method both appear fairly robust with respect to finding the breakpoint. We also compared several test statistics for deciding whether the data represent one line or two. A manuscript detailing this statistical subinvestigation will soon be submitted to a peer-reviewed journal.

References

Hu Q., T.J. Kneasfey, J.S.Y. Wang, L. Tomutsa, and J.J. Roberts, Characterizing unsaturated diffusion in porous tuff gravels. Vadose Zone Journal, 3 (4), 1425-1438, 2004.

SATURATED ZONE
FLOW AND TRANSPORT

This page intentionally left blank.

Determining the Redox Properties of Yucca Mountain-Related Groundwater Using Trace-Element Speciation for Predicting the Mobility of Nuclear Waste

James Cizdziel[1], Vernon Hodge[1], and Karen H. Johannesson[2]
[1]University of Nevada, Las Vegas | [2]University of Texas at Arlington

Research Objectives

The objective of this task is to determine the principal oxidation state (redox) species of select elements in samples of groundwater in the vicinity of Yucca Mountain, which is being evaluated as a site for geologic disposal of the nation's spent nuclear fuel and high-level nuclear waste. Samples to be analyzed include, but are not limited to, groundwater from wells of the Nye County Early Warning Drilling Program. Elements to be studied include arsenic (As), antimony (Sb), selenium (Se), chromium (Cr), manganese (Mn), copper (Cu), molybdenum (Mo), vanadium (V), tungsten (W) and uranium (U). Percentages of major redox species of these elements and total concentrations will be measured and tabulated.

The purpose is to develop a more accurate and complete description of the redox properties of Yucca Mountain-related groundwater, which influences the solubility and transport of radionuclides should they enter the groundwater system. A possible natural barrier to radionuclide migration in the saturated zone (SZ) is the presence of nonoxidizing or reducing environments. For example, the mobility of Tc-99 in oxic groundwater, ascribed to the pertechnetate ion, is greatly diminished in reducing groundwater. The containment of radionuclides away from the accessible environment is a key feature in the Yucca Mountain performance assessment.

Approach

In the current study, we have attempted to expand on previous work using multiple redox couples to generate an empirically based scale of redox conditions in Nye County groundwater. Although traditionally used to predict redox species in groundwater, E_h-pH relationships are based on thermodynamic concepts, and natural water systems are rarely in equilibrium. Moreover, some redox couples do not react on Pt electrodes at or near neutral pH values or at low concentrations. Thus there is some question as to how well by E_h-pH diagrams predict actual groundwater species. Indeed, a tentative thesis title for a graduate student working on the project is "How Well Do E_h-pH Diagrams Predict the Redox Species Distribution in Groundwater: Test Case: Southern Nevada." However, there are also challenges to measuring elemental oxidation states in groundwater, including sampling in a manner that preserves the native redox species, while employing suitable calibration standards and identifying interferences and artifacts in the analysis.

Our sampling approach has been to piggy-back sampling efforts to collect groundwater whenever other research or monitoring groups are pumping in the area. Samples are filtered, collected without headspace in a specially designed inert apparatus to minimize contact with the atmosphere, transported to the laboratory on ice, and analyzed as soon as possible to measure the native redox species. Field measurements, including E_h measurements from a Pt-electrode and other redox measures, are included for comparison purposes. Our analytical approach for the trace element redox analysis couples ion chromatography (to separate the ions) and inductively coupled plasma mass spectrometry (as an element selective detector). Multiple spikes and other QA measures are incorporated to assess data quality and to make sure on-column chemistry is not altering the redox species native to the groundwater.

Accomplishments

- The scientific investigation plan (SIP-UNLV-048) was reviewed and accepted in February 2006. Task personnel completed QA indoctrination and training. The task participated in the OCRWM Natural Barriers Thrust Area Project Review Meeting, held in Berkeley on February 13, 2006.

- An ion chromatograph was successfully coupled to two different inductively coupled plasma mass spectrometers. Scoping studies were performed to test procedures and optimize experimental parameters. Procedures for ten elements were tested using water from well J-12 on the Nevada Test Site (NTS). The method is published on the Nevada System of Higher Education's Quality Assurance Programs website.

- Altering the redox conditions of a mixed element standard revealed that vanadium (V) is particularly sensitive to redox changes using our

methodology. Thus, V, and potentially other elements, may serve as early indicators of subtle changes in the redox conditions of groundwater. Changes for less sensitive elements may suggest more drastic modification of the groundwater redox environment.

- A sample collection scheme was devised to minimize groundwater contact with air and preserve oxidation states native to the sample. Groundwater was collected from wells from the Nye County Early Warning Drilling Program (NCEWDP). This network of wells is generally located downgradient of Yucca Mountain in the Death Valley regional groundwater flow system. Samples were collected and analyzed from the following NCEWDP wells: 191M1 Zone 1 and 5, 1S Zone 1 and 2, and 9SX Zone 1-4. Additional sampling is planned for the NTS and Ash Meadows National Wildlife Refuge.

- Data from the NCEWDP wells indicate that most of the groundwater from these locations is oxidizing with respect to the elements measured. However, there also appear to be pockets of groundwater with reducing conditions (e.g., well 7SC, measured earlier). There is a minor trend with greater percentages of reduced species by depth within the same well. Using the measured values of the redox couples, together with field

measurements of pH, E_h values were calculated for comparison to field-measured values obtained by a standard Pt-electrode.

- A field-speciation method for arsenic, described in *USGS Water-Resources Investigations Report 02-4144*, was employed with slight modification at select sampling sites: 191M1 Zone 1 (unfiltered), 1S Zone 2 (filtered), 9SX Zone 1 (filtered), 9SX-Zone 4 (filtered). The results were comparable with data obtained by IC-ICP-MS, giving us increased confidence in our technique.

- Availability of oxidation state standards from qualified suppliers is extremely limited. Procedures were developed for the IC-ICP-MS analysis and for the acceptance of unqualified inorganic oxidation state calibration standards for quality-affecting work.

- The presentation "Redox Properties of Groundwater near Yucca Mountain Using Trace Element Speciation Determined by IC-ICP-MS" was given at the American Chemical Society National Meeting (3/21/07) at a special symposium entitled "Understanding Radionuclide Transport in the Environment: Remediation, Nuclear Waste Disposal and Long-Term Stewardship." A poster was also presented at the Devil's Hole Conference.

Field Studies for the Determination of Transport Properties of Radioactive Solutes and Colloids Using Chemical Analogues

Barry Freifeld[1], Paul Reimus[2], M. J. Umari[3], and Kathy Gilmore[4]

[1]Lawrence Berkeley National Laboratory (LBNL) | [2]Los Alamos National Laboratory (LANL)
[3]United States Geological Survey (USGS) | [4]Nye County Nuclear Waste Repository Project Office, Nye County, NV

Research Objectives

The objective of this program (hereafter referred to as the *in situ* Kd program) is to provide an enhanced understanding of saturated zone (SZ) radionuclide sorptive processes, resulting in refined estimates of transport rates along critical flow paths through volcanic tuffs south of the proposed Yucca Mountain repository. Based on relationships to be determined in the laboratory between sorptive behavior of radionuclides and appropriate chemical analogues, injection/pump back tests using analogues will be conducted in the field to observe in situ reactive transport processes. As a result of early observations performed at Borehole NC-EWDP-24PB (24PB) suggesting rapid SZ transport, the *in situ* Kd program shifted effort into the understanding of the fast flow paths encountered in 24PB. An emphasis was placed on the interpretation of data collected as a result of the logging and development of 24PB.

Approach

To further pursue a greater understanding of SZ processes, we developed a test bed for reactive transport sorptive studies. Specifically, the Nye County Nuclear Waste Repository Project Office drilled and completed Borehole 24PB in February and March of 2006. The 24PB testing program includes participation by staff from the Nye County Nuclear Waste Repository Project Office, Lawrence Berkeley National Laboratory, Los Alamos National Laboratory, and the United States Geological Survey. Borehole 24PB is located approximately 15 km south of the proposed Yucca Mountain repository and 6 km north of Highway 95 (Figure 1).

As part of the 24PB drilling program, geophysical logs (including gamma, formation resistivity, self-potential, single-point resistivity, and optical televiewer) were acquired. In addition to the standard suite of logs, flowing fluid electrical conductivity logs (FEC) and distributed thermal perturbation sensor (DTPS) logs were also acquired. The initial goal for collecting flowing FEC logs was to identify

hydrologically significant intervals for the placement of the U-tube groundwater sampling systems for reactive transport tests. The FEC logging program was planned to occur over one to two days. However, observations of fluid fluxes that were greater than expected led to the acquisition (between February 24 and February 28, 2006) of an extensive data set, consisting of six distinct tests comprising 30,000 ft of FEC logs collected over 32 runs. The DTPS logs were acquired to confirm the interpretation of the FEC logs.
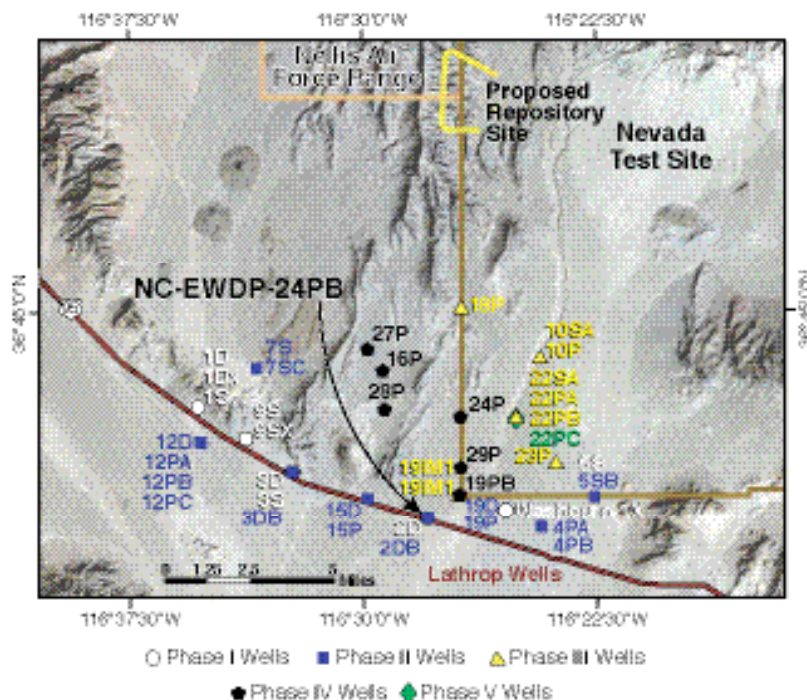

Figure 1. Location of Borehole NC-EWDP-24PB in the Amargosa Valley, approximately 15 km due south of the proposed repository site and 6 km north of Highway 95. Figure courtesy of Nye County NWRPO.

Accomplishments

The analysis of the FEC and DTPS data provides information not previously obtained from prior Yucca Mountain SZ characterization efforts. Accurate delineation of the spatial distribution of flow within a wellbore, coupled with well-constrained estimates for specific discharge, pro-

vides a comprehensive picture of local advective transport processes. Figure 2 shows DTPS data. The increase in temperature surrounding 24PB is plotted between 24 hours and 48 hours of heating. The fluid flux estimates shown in Figure 2 were produced using a numerical heat and mass-transport simulation that included both advective and diffusive heat-transport mechanisms. What is most significant in the top 125 m is the occurrence of two relatively thin high-flow zones, one at the water table (131–143 meters below ground surface) and the other towards the bottom of the Bullfrog Tuff (221–240 mbgs). Given that the fracture porosity for the Bullfrog Tuff is generally considered to be less than 1%, estimates for groundwater velocities in these fast flow zones are significantly greater than 10 km/yr.

To disseminate the results of this research to the wider scientific community, we gave a poster presentation at the 2006 AGU Fall Meeting in San Francisco, CA, as well as an oral presentation at the 2007 Devil's Hole Workshop, Death Valley, CA. It was emphasized that further investigation of the lateral extent of the identified fast-flowing pathways was required. In light of 24PB being close to where groundwater transitions from volcanics into an alluvial system, we believed that heterogeneities associated with this transition may be responsible for channeling groundwater into narrow geologic conduits. Still, given the implications of rapid transit of released radionuclides, and the close proximity of 24PB to the compliance boundary, further characterization of groundwater transport beneath and south of the proposed Yucca Mountain repository would seem to be warranted. With additional measurements of specific discharge and flow distribution, the current SZ model, based on the measured potentiometric surface, can be better calibrated, and significant reduction in uncertainty will be possible.
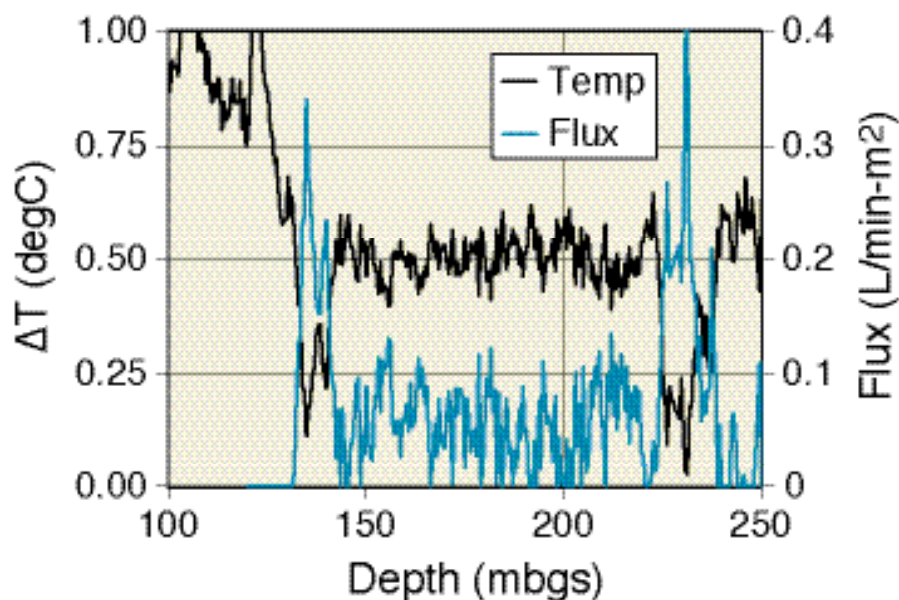

Figure 2. Acquired temperature data and estimated fluid flux for Borehole NC-EWDP-24PB. The groundwater table is located at 126 mbgs. Two distinct fast flow zones with large fluid fluxes are readily identifiable at the depth ranges between 131–143 mbgs and 221–240 mbgs.

Improved Characterization of Radionuclide Retardation in Volcanics and Alluvium

Cynthia A. Dean, Mei Ding, Paul W. Reimus, Cheryl Sedlacek, Schon Levy, and Steve Chipera
Los Alamos National Laboratory (LANL)

Research Objectives

The objective of this project is to demonstrate that uranium (U) and neptunium (Np) retardation in the saturated zone (SZ) is likely to be significantly higher than is currently assumed in Yucca Mountain Project (YMP) process models when slow desorption kinetics are considered. Secondary objectives are to investigate a possible correlation between hydraulic conductivity and sorption, and to study the effects of water chemistry and secondary mineralogy on the ability of the host rock to retard and/or attenuate radionuclides.

Approach

U and Np sorption to geologic media in current SZ models is based almost entirely on batch sorption and short-term desorption experiments that assume reversible, linear first-order kinetics. Only a single distribution coefficient (K_d) can be derived from such experiments, and stronger sorption sites with slower desorption kinetics tend not to be appropriately weighted because they are not effectively interrogated. To investigate the long-term desorption behavior of U and Np from Yucca Mountain saturated alluvium, specially designed column experiments were performed after one to fourteen days of batch sorption of U or Np to alluvium. Several alluvium and groundwater combinations were used in the experiments to study the effects of water chemistry and secondary mineral phases on radionuclide desorption behavior. Desorption rate constants estimated from these experiments were used to calculate a range of effective K_d values that account for strong sorption sites with slow desorption kinetics, while also accounting for less favorable U and Np sorption sites in the alluvium. Strong sorption sites are believed to be associated with smectite clays and zeolites in the alluvium, and the strength of sorption increases as carbonate concentrations in the groundwater decrease. These observations are consistent with a surface complexation sorption process that is suppressed by carbonate complexation in solution. An explicit kinetic model was developed to model the long-term desorption behavior and to corroborate effective K_d values obtained from the experimental data.

To investigate the role of clay minerals and water chemistry in Np sorption, we carried out batch sorption of Np to clays separated from Yucca Mountain alluvium in solutions of varying pH (6.5-10.2). To complement the batch sorption experiments, we conducted x-ray adsorption spectroscopic studies on the clay residue from the experiments to determine whether the Np had undergone any oxidation state changes during sorption.

To investigate a possible correlation between radionuclide sorption and saturated hydraulic conductivity, we also carried out U and Np batch sorption studies using alluvium from NC-EWDP-19PB, which was a sonic drill core hole. The saturated hydraulic conductivity of the material was measured by the Nye County Early Warning Drilling Program in large columns packed with alluvium from the same borehole intervals used in the batch experiments. Quantitative x-ray diffraction analysis and BET surface area measurements of the alluvium were also performed.

Accomplishments

During FY06, we completed U and Np long-term desorption experiments in the saturated alluvium. During the first quarter of 2007, we also completed interpretative modeling of the U and Np long-term desorption data for alluvium from NC-EWDP-19IM1A, 22SA and 10SA and groundwater from NC-EWDP-19D Zone 1 (lower carbonate), Zone 4 (higher carbonate) and NC-EWDP-10S. Relatively simple spreadsheet calculations provided the estimated ranges of effective partition coefficients ($K_{d,eff}$ values) in Table 1. These spreadsheet calculations were conducted in lieu of a more complex interpretive modeling approach, because there was insufficient time to qualify the software needed for a more complex model. Effective K_d values ($K_{d,eff}$) were calculated by dividing an upper and a lower bound sorption rate constant (K_{fmax} and K_{fmin}) by a desorption rate constant (K_r) calculated in two ways: a discrete method that sums the K_r values for each desorption sample multiplied by the fraction of radionuclide desorbed in each sample, and a binned method in which the desorption data is split into four mass fraction bins, and a numerical average K_r for each bin is calculated and multiplied by the fraction of radionuclide desorbed in that bin.

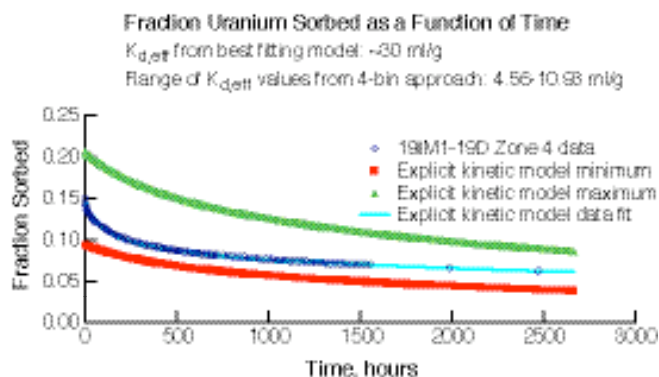To corroborate the $K_{d,eff}$ values derived from the spread-

Figure 1. Fraction of uranium sorbed to 19IM1A alluvium in 19D Zone 4 ground-water as a function of time. The red and yellow curves were calculated with the explicit kinetic model using a single $K_{f,min}$ or $K_{f,max}$ value in conjunction with the average K_r values from each of the four mass fraction bins assumed in the binned approach. The blue model curve (fit) was generated using the explicit kinetic model and allowing K_f and K_r to vary for each of the four mass fraction bins to obtain a best fit to the experimental data.

sheet calculations, an explicit kinetic model was developed to simulate four simultaneous sorption/desorption reactions, and therefore to determine if the sorption and desorption rate constants estimated from the four-bin approach described above yielded reasonable approximations to the fraction sorbed versus time in the desorption experiments. The red and yellow curves in Figure 1 were generated using the explicit kinetic model with the lower and upper bound rate constants, respectively, and the corresponding desorption rate constants were calculated from the binned experimental data. The blue model curve (fit) was generated using the explicit kinetic model, allowing the sorption and desorption rates for each of four sorption sites to vary independently until a best fit of the data was achieved. Figure 1 reflects the general trends observed

when going through this exercise for each of the data sets of Table 1. Batch sorption experiments of Np onto clays and subsequent x-ray absorbance near-edge (XANES) spectra of the Np-sorbed clay residue were completed in FY06. The results indicated that adsorption of Np onto clays increases as pH increases in solution. At pH 6.5 and 8.5, about 40% Np was adsorbed on clays. However, at pH 10.2, more than 90% of Np was removed from the solution. Note that the pH of the water was adjusted using HNO_3 and NaOH with no carbonate species added. The ionic strength of the water was controlled with NaNO3. XANES
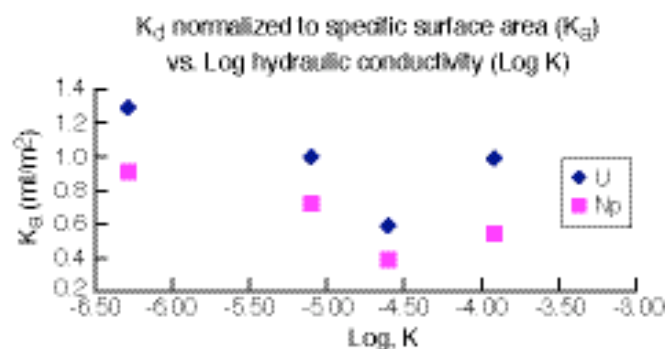

Figure 2. K_a (ml/m^2) plotted against Log K. The data suggest a weak correlation between hydraulic conductivity and sorption for U and Np.

spectra, and fitting results indicated that the Np sorbed at a solution of pH 10.2 was almost completely Np(V) which was the starting Np oxidation state in solution in all the experiments.

We also completed U and Np batch sorption experiments using four separate sonic-drill core alluvium samples from different depth intervals of NC-EWDP-19PB and groundwater from NC-EWDP-19D lower carbonate (shallow) zone. The results in Figure 2 indicate that a weak negative correlation exists between hydraulic conductivity and sorption of U and Np. The weakness of the correlation can possibly be attributed to a more fundamental dependence of sorption on alluvium mineralogy, with much of the apparent trend being explained by a secondary correlation between mineralogy and hydraulic conductivity. This secondary correlation results from the tendency for stronger sorbing clays and zeolites to be smaller-sized particles that are generally associated with lower saturated hydraulic conductivities.

Table 1. Effective $K_{d,eff}$ values from U and Np long-term desorption experiments

NC-EWDP Well No.	Groundwater/ Radionuclide	14 Day Batch Sorp.	$K_{d,eff}$ (ml/g) Discrete Min	Max	$K_{d,eff}$ (ml/g) Binned Min	Max
19IM1A	19D-Zone 1/U	5.22	65.83	280.72	62.57	266.81
19IM1A	19D-Zone 4/U	1.36	4.70	11.26	4.56	10.93
22SA	19D-Zone 1/U	9.96	36.14	80.03	45.01	99.69
22SA	19D-Zone 4/U	3.25	10.30	55.75	9.74	52.72
10SA	10S/U	5.17	17.98	23.62	17.63	23.16
19IM1A	19D-Zone 1/Np	10.12	99.77	242.15	96.55	234.35
19IM1A	19D-Zone 4/Np	5.75	40.12	128.27	41.49	132.66
22SA	19D-Zone 1/Np	23.31	160.10	463.94	158.06	458.02
22SA	19D-Zone 4/Np	17.87	109.42	332.95	108.57	330.35

Carbon-14 Groundwater Analysis

Gary L. Patterson[1] and James Thomas[2]

[1]United States Geological Survey (USGS) | [2]Desert Research Institute

Research Objectives

The current range of groundwater travel times being used in performance assessment modeling of Yucca Mountain is overly conservative, because of the uncertain age estimates available using traditional dissolved-inorganic-carbon (DIC) groundwater dating techniques. The objective of this work is to provide improved estimates of groundwater ages along flow paths downgradient from Yucca Mountain. Improved ages can be used to provide more realistic estimates of the time required for any potential contaminants to reach the accessible environment.

Approach

The approach to this problem involves the measurement of carbon-14 (^{14}C) activities in both dissolved inorganic carbon (DIC) and dissolved organic carbon (DOC) in groundwater from wells located along flow paths emanating from Yucca Mountain. Traditional DIC radiocarbon dating assumes that the ^{14}C percent modern carbon (pmc) acquired during recharge through the soil zone only changes along a flow path as a result of radioactive decay of ^{14}C. This assumption is not completely valid when the aquifer material contains carbonates having 0 pmc ^{14}C activity ("dead" carbon) that can be isotopically exchanged into the water. Radiocarbon dating of DOC has the advantage of not requiring corrections based on assumed models of water-rock interaction. Like DIC, DOC is acquired from the soil zone during recharge; however, little ^{14}C-bearing DOC is expected to be present in aquifer materials along flowpaths. Thus, radiocarbon dating of DOC should give a direct measure of the amount of time elapsed since the groundwater entered the system.

Both sets of measurements, along with ^{13}C-DIC, ^{13}C-DOC, and hydrochemical modeling, are used to more accurately estimate the age of groundwater. The USGS computer program NETPATH was used to model the changes in groundwater chemistry along potential flowpaths and to assess mixing of different waters.

Accomplishments

The chemical and isotopic content of groundwater in the vicinity of Yucca Mountain was used to identify areas forming six relatively distinct hydrochemical facies: Western Yucca Mountain, Eastern Yucca Mountain, Fortymile Wash, Bare Mountain, Amargosa River, and Eastern Amargosa Valley (Figure 1). The general hydrochemical relations within these facies, along with generalized flow paths determined from hydrochemical and hydrologic information (Figure 2), were used to guide the NETPATH modeling.
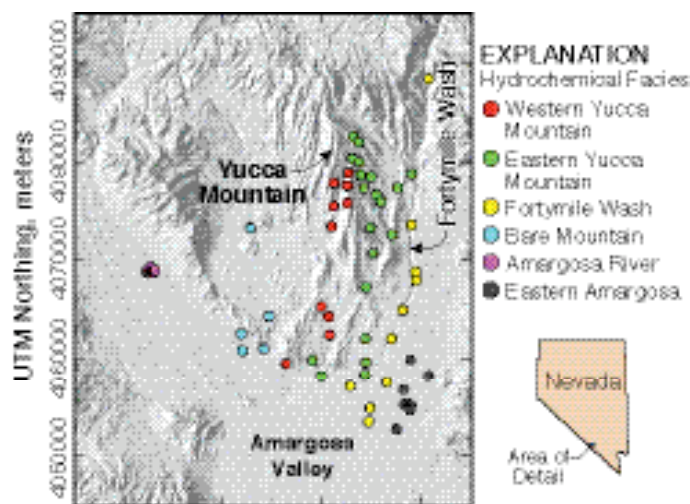

Figure 1. Hydrochemical facies in groundwater samples in the Yucca Mountain vicinity (wells in text will be labeled).

Wells located within the Fortymile Wash facies were used to assemble hypothetical end-member flowpaths and several mixing flowpaths. Water from the two wells at the north end of the wash, UE29a#1 and UE29a#2, have deuterium (δD) values that are too heavy relative to any of the downgradient Fortymile Wash facies wells to be the sole source of these downgradient waters. Similarly, water from well NC-EWDP 02D at the south end of the facies is isotopically much lighter than the other Fortymile Wash facies wells in the vicinity, so it also must represent a mixture of waters. Furthermore, waters from UE29a#1 and a#2 have δ^{13}C values that are isotopically light in comparison to water in wells along the Fortymile Wash flowpath. NETPATH modeling of these three wells did not produce satisfactory results as end-member waters with or without

mixing with other Fortymile Wash groundwaters. This indicates that upper Fortymile Wash groundwater mixes with groundwaters from other facies as it moves downgradient to the south.
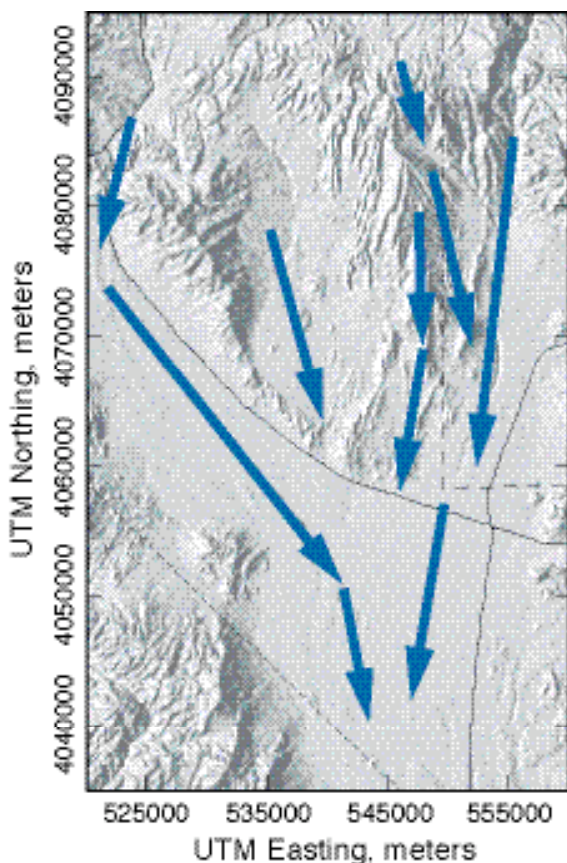

Figure 2. Generalized groundwater flow paths identified from hydrochemical and isotopic parameters.

Mixing Fortymile Wash facies water with water from the Eastern Yucca Mountain facies produced more satisfactory geochemical models. For example, mixing water from UE29a#2 with waters from WT-3 and NC-EWDP 10P-zone-1 successfully simulated the hydrochemical characteristics of water from NC-EWDP 02D. Models of mixtures of Fortymile Wash and Eastern Yucca Mountain groundwaters yield calculated travel times of 2,000 to 4,000 years.

Wells located within the Eastern Yucca Mountain hydrochemical facies were used to assemble hypothetical end-member flow-path groundwaters and several mixing flow-

paths. For the nonmixing simulations, well WT-24 served as the northernmost end-member of the Eastern Yucca Mountain facies. Models successfully simulated flow from WT-24 to H4, but models from H4 to WT-3, WT-12, WT-17 or NC-EWDP 18P were not successful, due to large differences between observed and modeled δD, $\delta^{13}C$, and/or mineral mass-transfer values. These differences may indicate the need to add recharge as a mixing component along these potential flow paths.

Several nonmixing flowpaths were simulated for wells in the Western Yucca Mountain facies. Flowpaths from H5 to SD-6 and H5 to WT-10 were successfully simulated and resulted in calculated travel times of approximately 2,500 and 3,500 years, respectively. Models that failed to simulate downgradient chemistry include WT-10 to NC-EWDP 28P, and WT-10 to NC-EWDP 16P. Additional models for the southern end of the facies include H6 to NC-EWDP 9SX, which had excessive mass transfer of silica, and H6 to NC-EWDP 12PA, which required excessive exchange to match measured and modeled $\delta^{13}C$ values. The unsuccessful models may indicate the need to add recharge as a mixing component for these flow paths. Two mixing models successfully simulated downgradient chemistry. These models represent a mixture of groundwater from well H5 and well SD6, flowing to well WT-10; and a mixture of groundwater from wells H5, H6, and WT-10 flowing to well NC-EWDP 3D.

Although preliminary, the results of the hydrochemical modeling effort are important, in that flow paths from north to south within the Western Yucca Mountain facies and from the Eastern Yucca Mountain facies into Fortymile Wash were successfully simulated. Simulations that failed to adequately represent the groundwater chemistry also are valuable and in many cases may indicate that local recharge may be a substantial component of groundwaters, particularly in alluvial wells. Travel times of 2,500 to 3,500 years between particular wells in the Western Yucca Mountain facies, and 2,000 to 4,000 years for mixtures of Fortymile Wash facies and Yucca Mountain facies groundwaters, may allow more accurate estimates of travel time from Yucca Mountain to the accessible environment. Travel times for other more hypothetical flow paths and mixtures of waters produce a range of about 1,000 to 6,000 years using Nye County wells as the end points of flow paths. More detailed assessment of groundwater travel times from directly beneath the proposed repository is not currently possible, because little ^{14}C-DOC data are available for groundwater beneath Yucca Mountain.

This page intentionally left blank.